Journal of Energy Storage 110 (2025) 115197

Contents lists available at ScienceDirect

Journal of Energy Storage

journal homepage: www.elsevier.com/locate/est

Research papers

Uncertainty-aware energy storage investment planning through arbitrage in DA and RT markets using novel block orders

A. Belmondo Bianchi *, H.H.M. Rijnaarts, S. Shariat Torbaghan

Environmental Technology, Wageningen University and Research, Building 118, Bornse Weilanden 9, Wageningen, 6708 WG, Gelderland, The Netherlands

ARTICLE INFO

Keywords:
Energy storage investment planning
Market participation strategy
Flexibility block orders
Distributionally robust optimization
Chance constraints

ABSTRACT

Energy Storage Systems (ESS) represent capital-intensive technologies set to play a pivotal role in the future energy landscape. In competitive markets, ESS rely heavily on cross-temporal energy arbitrage within day-ahead markets and across multiple segments, such as day-ahead to real-time markets. However, their revenue potential is heavily reliant on the accuracy of renewable energy generation forecasts, such as wind forecasts, which can influence market prices. This dependence can hinder the integration and development of ESS technologies. To address this challenge, this study presents a novel investment planning and participation strategy framework for ESS market engagement. The framework formulates the problem as a distributionally robust chance-constrained program, approximating it as a deterministic mixed-integer second-order cone program. To mitigate the impact of imperfect wind forecast uncertainties, we introduce two innovative block orders that facilitate ESS order clearing based solely on price spread, preserving convexity and computational efficiency. Numerical findings demonstrate the effectiveness of the proposed block orders in enabling energy arbitrage in the day-ahead and real-time markets in the presence of imperfect wind forecasts. The proposed model can identify the optimal investment and operational strategy, hedging system operators against wind power generation uncertainty while offering ESS investors a safety margin on the recovery of their investment.

1. Introduction

1.1. Background and motivation

The energy landscape is undergoing a transformative shift driven by the urgent need for sustainable and resilient power systems [1]. With the growing penetration of Renewable Energy Sources (RES) and the increasing electrification of various sectors, the efficient storage of energy has emerged as a critical component in meeting the demands of a rapidly evolving market [2]. Energy Storage Systems (ESS) hold the key to overcoming the intermittency and variability of renewable energy generation while offering flexible, reliable, and clean power supply solutions [3].

The integration of ESS in the power network offers a means to store excess energy generated from RES during periods of high production and release it back into the system during periods of high demand or low RES availability [4]. The stored energy can be dispatched and utilized to stabilize grid frequency and voltage, ensuring the stability and reliability of the power network [5]. This capability enhances the overall flexibility of the power system, enabling better balancing of electricity supply and demand and mitigating the effects of intermittent energy generation from RES [6]. Moreover, the integration of ESS provides opportunities for Demand Response (DR) programs, where consumers can actively adjust their electricity consumption patterns based on pricing or other incentive mechanisms [7,8]. This demand-side flexibility, combined with ESS, enables more efficient utilization of energy resources and further enhances the overall reliability and resilience of the power system [9].

However, ESS are capital-intensive technologies. Private sector investments are crucial to achieving the level of ESS integration that is needed in the future. In a competitive market environment, cross-temporal and/or cross-segment energy arbitrage in Day-Ahead (DA) and/or across DA and Real-Time (RT) markets are considered as the main market participation strategies ESS implement [10]. The problem is, that such participation strategies are highly sensitive to imperfect price forecasts [11]. The problem is, the market prices are becoming increasingly volatile (and therefore harder to forecast), as the share of RES is growing in the power systems. Consequently, the economic viability of ESS through energy arbitrage has become increasingly challenging and associated with higher risks [12]. This, in turn, undermines the financial justification for investment by private entities, leading to heightened hesitation among private investors to commit to new ventures in this sector [13]. This in turn can impede private investment

* Corresponding author.
E-mail address: alessio.belmondobianchidilavagna@wur.nl (A. Belmondo Bianchi).

https://doi.org/10.1016/j.est.2024.115197
Received 10 September 2024; Received in revised form 6 December 2024; Accepted 24 December 2024
Available online 8 January 2025

Nomenclature

Abbreviations

BOs	Block orders
$CVaR$	Conditional value-at-risk
DA	Day-ahead
DBO	Day-ahead block order
DR	Demand-response
$DRCC$	Distributionally robust chance-constraints
$DRCCP$	Distributionally robust chance-constrained program
DRO	Distributionally robust optimization
ESS	Energy storage system
FBO	Flexibility block order
$MIQP$	Mixed-integer quadratic program
$MISOCP$	Mixed-integer second-order cone program
MO	Market operator
RES	Renewable energy sources
RT	Real-time
$SBSO$	Scenario-based stochastic optimization
SOC	Second-order cone
VPP	Virtual power plant

Number sets

$\mathbb{R}$	Real numbers
$\mathcal{E}$	Power lines
$\mathcal{G}$	Conventional power generators
$\mathcal{L}$	Conventional power loads
$\mathcal{N}$	Power buses
$\mathcal{S}$	Energy storage units
$\mathcal{T}$	Number of time slots
$\mathcal{W}$	Wind power generators
$\mathcal{Z}$	Number of random variables
Π	Ambiguity set

Parameters

ϵ	Violation probability level for individual DRCCs
ϵ'	Confidence level for SOC approximation of DRCCs
η_s^{ch}, η_s^{dc}	Charging and discharging efficiencies of storage s
γ_t	Aggregated wind forecast error at time t
$\hat{q}_{w,t}^W$	Forecast of wind generator w at time t
μ^{Π}	Mean vector of forecast errors
ϕ^T	Transpose of a vector of ones
Σ	Covariance matrix of forecast errors
Σ_t	Diagonal sub-matrix t of Σ
$\tilde{\lambda}_t$	Day-ahead price forecast at time t
$\underline{f}_{n,m}, \overline{f}_{n,m}$	Lower and upper flow limits for line (n,m)
$\underline{Q}_g^G, \overline{Q}_g^G$	Lower and upper power bounds for generator g
$\underline{Q}_{l,t}^L, \overline{Q}_{l,t}^L$	Lower and upper power bounds for load l at time t
$\underline{Q}_{w,t}^W, \overline{Q}_{w,t}^W$	Lower and upper power bounds for wind generator w at time t
$B_{n,m}$	Susceptance of line from bus n to bus m
C_g^{Av}, C_s^{Av}	Energy-to-flexibility spread for generator g and storage s
I_s^0, I_s^E, I_s^Q	Cost factors for initial investment, energy rating, and power rating of storage s
M	Big-M factor
p_g^G	Marginal production cost of generator g
$p_{l,t}^L$	Bid price for load l at time t
p_s^{spr}	Minimum price spread for DBO activation

Variables

$\alpha_{g,t}, \beta_{s,t}$	Flexibility offered by generator g and storage s at time t
$\breve{e}_{s,t}$	Uncertainty-dependent state of energy of storage s at time t
$\breve{q}_{s,t}^{ch,D\to R}$	Uncertainty-dependent FBO charging factor for storage s at time t
$\breve{q}_{s,t}^{ch}$	Real-time charging factor for storage s at time t
$\breve{q}_{s,t}^{dc}$	Uncertainty-dependent FBO discharging factor for storage s at time t
Δ_t	Random forecast error vector at time t
$\hat{\theta}_{n,t}, \breve{\theta}_{n,t}$	Nominal and uncertainty-dependent voltage angle at bus n at time t
$\hat{e}_{s,t}^{D\to R}$	Nominal state of energy for storage s at time t (FBO)
$\hat{e}_{s,t}^{D}$	Nominal state of energy for storage s at time t (DBO)
$\hat{f}_{n,m,t}, \breve{f}_{n,m,t}$	Nominal and uncertainty-dependent power flow from bus n to bus m at time t
$\hat{q}_{g,t}^G, \breve{q}_{g,t}^G$	Nominal and uncertainty-dependent power output of generator g at time t
$\hat{q}_{l,t}^L$	Power demand of load l at time t
$\hat{q}_{s,t}^{ch,D\to R}$	Nominal FBO charging for storage s at time t
$\hat{q}_{s,t}^{ch,D}$	DBO charging for storage s at time t
$\hat{q}_{s,t}^{ch}$	Total day-ahead charging for storage s at time t
$\hat{q}_{s,t}^{dc}$	DBO discharging for storage s at time t
$\mathbb{P}$	Worst-case uncertainty distribution
$\omega_{i,t}$	Forecast error for renewable generator i at time t
$\overline{E}_s$	Maximum energy rating of storage s
$\overline{Q}_s$	Maximum power rating of storage s
e_s^0	Initial state of energy of storage s
U_s	Binary variable for storage investment decision

which can lead to flexibility shortage and from there, severe operational issues in transmission and distribution networks [14]. To exploit the full potential of ESS, an adequate mechanism that ensures investment recovery needs to be put in place [15]. Such a mechanism provides a steady and reliable revenue stream and ensures the economic prosperity of such risky investments.

Efforts are made to hedge the investors and to ensure investment recovery from the inherent market risks ranging from introducing novel storage policies (in terms of financial support schemes) to improving forecasting accuracy [9,16]. The issue with support policies is that they can easily lead to a large financial burden on the consumers. Moreover, such policies can be affected by the political atmosphere and therefore, are not considered financially sustainable in the long

run [17]. Despite significant efforts by researchers to enhance the accuracy of predictions, forecast error remains unavoidable and cannot be entirely eliminated [18]. Consequently, the development of a robust investment promotion mechanism remains an unresolved challenge [19]. Addressing this gap is the primary objective of this research.

1.2. Research gaps

ESS technologies, such as batteries, pumped hydro storage, and hydrogen, differ significantly in terms of investment costs, capacity, lifetime, storage losses, efficiency, ramping rates, and reaction times [20,21]. Studies show that there is no universally ideal ESS technology since the choice depends on the specific characteristics of the power system and the availability of RES [22]. Determining the optimal storage technology, location, and capacity is a complex and context-dependent task due to the need to balance operating costs, investment costs, and benefits while considering various short- and long-term uncertainties. Consequently, decisions regarding the adequate ESS capacity to invest in, and the optimal operational strategy to participate in a dynamic market environment, should be made with care. Such complex decision-making problems can be well formalized and solved using mathematical optimization [14,23,24].

Considering electricity market dynamics is critical in assessing optimal ESS investment and operational decisions [19]. In this context, market dynamics refer to factors influencing price fluctuations, supply–demand equilibrium, and the behaviour of producers and consumers [15]. These dynamics manifest as price volatility and price spikes, resulting from complex inter-temporal dependencies and strategic market manipulation by participants [25]. Neglecting these dynamics can compromise the robustness of investment and operational decisions. However, incorporating these dynamics presents challenges due to the computational complexity of considering a full temporal horizon, typically spanning one year, within a stochastic programming optimization framework [26]. This complexity arises from the high-dimensional state space and the need to account for multiple sources of uncertainty in a temporally coupled decision-making process.

Several studies have focused on optimizing ESS as flexible resources for participating in various electricity market transactions [27]. Previous research has primarily addressed scheduling ESS paired with RES in the electricity market, considering uncertainties such as prices, loads, and RES [28]. A common technique to model these uncertainties is Scenario-Based Stochastic Optimization (SBSO) [29]. For instance, [30] proposed an SBSO model for ESS participation in the DA market under different uncertainties, showing the potential for ESS integration and its strategic behaviour in influencing prices. However, they did not consider ancillary services in the RT market. Another study, [31], introduced a bi-level programming framework optimizing DA prices and RT imbalance costs, considering the coordination of price-making Virtual Power Plants (VPPs) and ESS under RES uncertainty. They demonstrated that ESS plays a significant role in reducing RT imbalance costs, increasing RES integration, and enhancing system stability. One possible limitation of the above studies is that uncertainty is modelled using the SBSO approach. This approach can become computationally expensive due to the need for numerous scenarios derived from probability distributions, especially as the number of uncertain sources increases or scenarios become more complex. This complexity makes it difficult to consider complex market dynamics within the optimization framework while maintaining computational efficiency. In such cases, alternative uncertainty modelling techniques, such as Distributionally Robust Optimization (DRO), can be considered [32,33].

The work in [29] proposes a data-driven DRO method for scheduling ESS. It considers ESS participation in both DA and RT markets, addressing uncertainties in prices, demand, and generation. They use the Wasserstein metric for risk-based portfolio optimization, reformulating the problem as a finite convex problem based on Conditional Value-at-Risk (CVaR). Results show improved out-of-sample performance despite higher computational effort compared to moment-based DRO. In [34], an uncertainty-aware DRO model for ESS in the intraday market is introduced. This study develops a novel algorithm to solve the DRO problem and compares distance-based and moment-based DRO. Their study demonstrates the effectiveness of their approach in integrating ESS to mitigate the variability of RES while considering operational constraints and market participation. However, the aforementioned studies focus on the operational constraints and market participation strategies of ESS without addressing optimal investment planning, thereby overlooking the trade-offs between operational and investment decisions.

In addition to the short-term scheduling and operational problems previously discussed, several studies have addressed long-term ESS investment decisions. For instance, [35] proposed a robust planning-operation decomposition methodology for optimal ESS location, selection, and operation in mid-to-low voltage distribution networks, demonstrating benefits such as grid congestion management and reduced energy losses. However, this approach did not account for uncertainties in renewable generation, demand, and energy prices, limiting its practical applicability. The work in [36] developed a distributionally robust capacity sizing method for renewable generation, transmission, and storage using a Wasserstein distance-based ambiguity set to model RES uncertainties. Their method balances robustness and computational efficiency compared to SBSO. Yet, it excluded ESS market participation, which may introduce additional computational complexity and restrict applicability, especially for large-scale problems. Similarly, [37] introduced a DRO model for ESS planning that utilizes a Wasserstein metric to address worst-case supply and demand uncertainties. This framework highlights the impact of market prices on ESS planning and shows advantages over SBSO and Robust Optimization (RO). However, it does not consider market participation, such as bidding behaviour and ESS order clearing, which are crucial in a competitive market structure. While these studies contribute significantly to the field of ESS investment decision-making, they each exhibit limitations in addressing uncertainties and market participation.

To bridge this gap, a promising solution for hedging various ESS technologies against market uncertainties is to utilize Block Orders (BOs). In the context of European markets, BOs are specialized order types that encompass multiple orders. BOs make the acceptance of one order type dependent on another. They allow traders to combine multiple time units into a single order. If BOs are accepted, they are executed on an all-or-none basis, meaning either all hours in the order are executed at the determined price or the entire order is rejected. There are four BO types: regular block orders (a single order that spans over multiple consecutive time steps, all at the same price and volume), profile block orders (where there are different volumes for each hour within the block, with a minimum acceptance ratio), curtailable blocks (which allow traders to define a minimum acceptance ratio above which a block order is accepted), and loop blocks (a family of two blocks executed or rejected together) [38–40].

Due to their nature, the inclusion of complex BOs necessitates the introduction of integer variables in the modelling of the optimization algorithm used for market clearing. This, in turn, transforms the original problem into a Mixed-Integer Quadratic Programming (MIQP) problem, which is computationally challenging to solve even under deterministic conditions [41]. The challenge intensifies when uncertainties arising from imperfect forecasts are incorporated into the decision-making process. Addressing these uncertainties typically requires solving the MIQP problem [42] across a large number of scenarios in SBSO or incorporating the uncertainties into constraints in an RO formulation, both of which become particularly cumbersome in the presence of binary variables. This highlights the need for an alternative modelling approach that retains the benefits of binary orders while enabling the seamless integration of uncertainty into the decision-making framework.

As we demonstrate later in this paper, the new BOs introduced here address this need by modelling loop orders using continuous variables. Notably, the proposed BOs are applicable to non-ideal energy storage systems with charging and discharging efficiencies below 100%. This characteristic ensures the avoidance of simultaneous charging and discharging without the need for introducing binary variables. It is important to note that, assuming the proposed BOs are implemented, the market clearing results will be the same as in the case where loop orders are used. In this case, the binary variables first decide which orders to accept, while the continuous variables determine the portion of each order to be accepted. This is demonstrated in [43,44].

To summarize, previous works have examined ESS participation in electricity markets, primarily focusing on short-term scheduling and operational decisions, such as economic dispatch, while often neglecting long-term investment considerations. When long-term investments are addressed, as in [37], the model tends to oversimplify critical operational aspects, including market clearing mechanisms, bidding behaviour, and ESS order clearing. This simplification restricts the model's ability to capture the full dynamics of electricity markets. One reason for this could be that, in most works, uncertainty is often managed using methods such as SBSO and distance-based DRO. These approaches can become computationally demanding as a larger set of factors influencing the long-term investment and short-run operational decision are considered; hence, the state-space dimensionality increases, particularly when integrating discrete investment decisions with temporally coupled operational decisions [45,46].

As highlighted in [47], moment-based Distributionally Robust Chance-Constrained (DRCC) optimization offers potential advantages over SBSO and distance-based DRO. It accommodates diverse risk preferences and reliability assessments of ESS under uncertainty without relying on specific probability distribution assumptions, while maintaining computational efficiency across various problem types and sizes. This presents a research opportunity to develop a moment-based DRCC approach that integrates the investment and operational decisions of an ESS in a competitive market setup while maintaining computational efficiency.

1.3. Scope and contributions

This work proposes a novel DRCC optimization framework to evaluate the optimal investment planning and the optimal (dis)charging dispatch of a generic ESS. The problem is formulated as a Mixed-Integer Second-Order Cone Program (MISOCP) subject to RES generation uncertainty in a power transmission network. It aims to identify the optimal storage investment and operational strategy that ensures a return on investment while maximizing the overall utility of the power system by enhancing its flexibility, efficiency, and stability. The novelty of this work lies in the development of a moment-based DRCC optimization framework that integrates long-term planning with day-ahead scheduling and real-time operation in the electricity market. The investment and operational decisions are considered interdependent and given equal emphasis because the economic viability of storage investments is contingent upon trading revenues and the given market structure. To this end, this research introduces novel BOs, namely Day-Ahead Block Orders (DBOs) and Flexibility Block Orders (FBOs), designed for flexible units such as ESS to engage in temporal and cross-market energy-to-flexibility arbitrage.

To the best of the authors' knowledge, this study represents the first instance where a DRCC framework has been applied to evaluate ESS investment planning and market participation incorporating such BOs. This work provides valuable insights into optimizing both investment planning and operational strategies for ESS in the face of RES uncertainty. The contributions of this study are threefold:

1. proposes a novel energy storage investment planning framework for non-ideal energy storage systems in both long-term investment planning and short-term (hourly) operation, formulated as a DRCC-MISOCP, that integrates day-ahead and real-time electricity market participation under wind power generation uncertainty. The proposed modelling approach introduces binary variables for long-term investment modelling while modelling the short-term uncertainties using the novel BOs.
2. introduces novel block orders, namely DBOs and FBOs, which enable storage units to engage in temporal and cross-market energy to flexibility arbitrage. The BOs allow storage investors to externalize their risk related to imperfect forecasts in terms of the arbitrage spread within the DA market and across the DA and RT markets without jeopardizing market competitiveness. The introduction of these BOs eliminates the need for binary variables in storage participation. From a modelling perspective, the proposed approach decouples the constraints involving binary variables related to long-term investment decisions from those that include chance constraints to address short-term uncertainties.
3. demonstrates the potential for recovering storage investments through market participation while offering investors and system operators a hedge against wind power generation uncertainty under different risk preferences.

1.4. Organization

The rest of this paper is organized as follows. Section 2 introduces the modelling framework for ESS investment and market participation strategy, including the novel DBOs and FBOs proposed in this study. Additionally, it details the modelling assumptions and formalizes the DRCC problem formulation, outlining the reformulation procedure that leads to a tractable optimization problem. Section 3 presents the complete tractable formulation of the DRCC-based long-term investment planning for storage technologies participating in competitive market environments through the specified block orders. Section 4 provides the numerical results, demonstrating the effectiveness of the proposed approach. Finally, Section 5 concludes the paper and outlines avenues for future research, highlighting potential enhancements and applications of the proposed framework.

2. Storage investment and market participation

2.1. Novel block orders

The DA and RT are two distinct segments, each serving a different purpose in the electricity market. Decisions made in the DA market are based on forecasts, while the RT market serves to correct these decisions as new, real-time information becomes available. In Europe, the DA market is operated by EPEX, while the RT market is managed by the Transmission System Operator (TSO). In this context, storage systems can participate in both markets, primarily making money through arbitrage. This means they can buy electricity at lower prices in the DA market and sell it at higher prices in the RT market, profiting from the price differences between the two timeframes.

For energy storage systems, the situation can be more complex. ESS may need to purchase energy in the DA market to deliver it to the TSO in the RT market, especially if wind generation is overestimated in the DA forecast. Conversely if wind generation is underestimated in the DA market, the ESS should avoid charging in the DA market to reserve capacity for charging in the RT market. However, this latter scenario is not considered in the context of this work, as over-prediction of wind (and thus underproduction in the RT market) typically results in an aggregate generation deficit, creating an imbalance that flexibility sources must address. Excess wind generation can be curtailed to manage this imbalance.

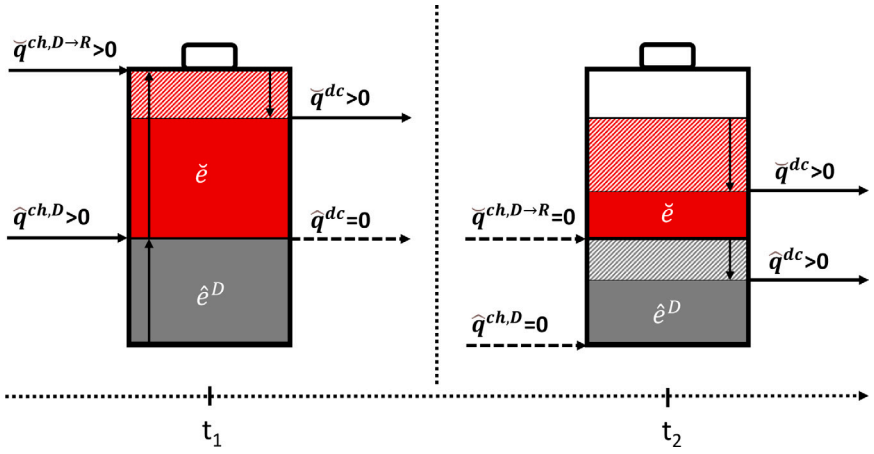

Fig. 1. Storage charging and discharging operations based on DBO and FBO working principle.

Therefore, as a follow-up to [43], here we examine two market products: DBOs and FBOs. These orders are similar to loop orders in that they allow the bundling of buy and sell block orders. That is, given the complexity of modelling such decisions in an uncertain environment, we propose introducing two novel market products to facilitate such trades for the special case of non-ideal energy storage systems: (1) DBO (a cross-temporal product within the DA market), (2) FBO$^-$ (a cross-market product from DA to RT), and (3) FBO$^+$ (a cross-market and time product). These new products are designed to enable more efficient decision-making and trading in the presence of uncertainties, particularly for energy storage systems.

The difference is that these products are specifically designed to hedge ESS investors against the risks associated with the mentioned uncertainties, without compromising the competitiveness of the market. The DBOs are similar to those introduced in [43]. What makes them different from loop orders is the way they are designed; there is no need to define a binary order associated with the acceptance or rejection of buy and sell orders. These orders have been shown to alleviate risks associated with DA price forecasts encountered by price-taker storage units engaged in cross-temporal energy arbitrage in the DA market [43]. Likewise, the FBOs are loop orders that span various times. What makes them different from loop orders is that they span different segments of the electricity market (i.e., DA and RT). The FBOs enable price-taker storage units to participate in cross-market and temporal energy-to-flexibility arbitrage. Essentially, FBOs allow a flexible unit (such as storage) to procure energy in the DA market and provide it as flexibility services in the RT and/or ancillary market at the same or different time instances.

2.1.1. Working principle

To illustrate the working principle of the proposed DBOs and FBOs, Figs. 1 and 2 visualize these two BOs from the ESS and the market viewpoints. Consider a storage unit engaging in the DA market with the objective of optimizing its participation in the RT market. Let us simplify by assuming there are only two time instances, labelled as t_1 and t_2. We will also assume that the DA trades are solely financial, and the final operational strategy will be determined by trades made in the DA market and adjustments in the RT market based on real-time system requirements.

Now let us examine t_1. Suppose the storage plans to charge a certain amount $\hat{q}^{ch,D} > 0$ at time t_1 to be traded exclusively in the DA market later. Additionally, let us suppose the storage plans to charge $\breve{q}^{ch,D\to R} > 0$ to be traded in the RT. The latter represents a flexibility service that the storage unit commits to providing during the DA scheduling, to be delivered in the RT market. Consider a scenario where, during real-time operation, a deficit in total RES production is observed at time instance t_1 in the system, attributed to an imperfect forecast. In reaction, the storage system chooses to charge less than planned in the DA schedule. This equates to discharging $\breve{q}^{dc}$ in the RT. Hence, the actual charging rate is determined by $\breve{q}^{ch,D\to R} - \breve{q}^{dc} \geq 0$. Under these circumstances, a portion of the capacity reserved in the DA for RT is left unallocated, resulting in a lower state of energy in the RT ($\breve{e}$). This is referred to as negative flexibility block order (FBO$^-$).

Now, let us examine t_2. The electricity stored during t_1 in the DA is discharged (i.e., $\hat{q}^{dc} > 0$), leading to a reduction in the DA state of energy of the storage ($\hat{e}^{D}$). This phenomenon is known as cross-temporal DA arbitrage (DBO). Suppose another RES deficit is observed at t_2 in real-time. As a response, additional energy is discharged (i.e., $\breve{q}^{ch,D\to R} - \breve{q}^{dc} < 0$), resulting in a decrease in the RT state of energy of the storage ($\breve{e}$). Here, $\breve{q}^{dc}$ represents a genuine discharging event in RT using the energy stored in t_1 (note that $\breve{q}^{ch,D\to R} = 0$). This is referred to as positive flexibility block order (FBO$^+$).

Fig. 2 shows the positioning of the energy storage in the DA and RT with a DBO, FBO$^+$ and FBO$^-$. From the market viewpoint, if the DBO is accepted, it implies that the storage charges the energy at the 8–9 time slot and discharges it at 17–18 both in the DA market. Likewise, if the FBO$^+$ is accepted, it leads to a charging at 4–5 in the DA and a discharge at 20–21 in the RT market. And if the FBO$^-$ is accepted, it involves withdrawing a planned charging action that was committed in the DA market, where the charged energy was intended to be used as a flexibility service in the RT market.

The primary advantage of the proposed DBOs and FBOs lies in the bidding process. For DBOs, the storage unit only requires knowledge of the minimum price spread at which is willing to engage in DA arbitrage. Conversely, for FBOs, the storage operator only needs information about the minimum energy-to-flexibility spread. In the following Section, 2.2, we provide the modelling assumptions used in this study.

2.2. Modelling assumption

2.2.1. Market structure

This paper examines the optimal investment planning and market participation strategy of an ESS participating in the market. We consider a competitive market structure that is cleared in a centralized manner by the global Market Operator (MO). The MO is assumed to possess complete information and aims to clear the market efficiently. The market clearing problem is formulated as an optimization algorithm that aims to minimize the aggregated social cost of the market while adhering to the operational constraints of the power system, including the supply units (i.e., generators and wind producers), loads, and storage systems. The upper/lower bounds of these constraints are represented in the form of standard bid orders (for normal assets), as well as the DBO and FBOs introduced earlier (for storage units).

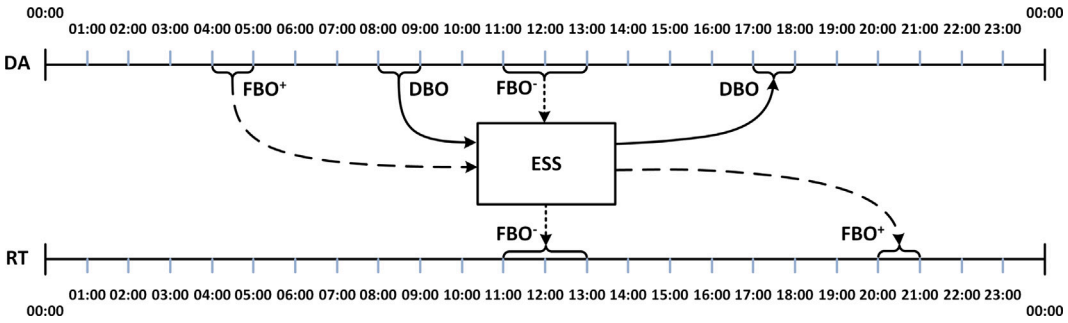

Fig. 2. Positioning of the ESS in the DA and RT markets, highlighting the working principles of DBOs and FBOs for cross-temporal and cross-market arbitrage.

It is important to note that, in addition to the market participation strategy, the proposed framework seeks to identify the optimal storage investment decision with respect to ESS capacity and its location within the network. This is achieved by identifying the break-even point, which is the investment capacity at which storage revenues from energy arbitrage are equal to the investment cost of constructing the storage. For simplicity, factors such as inflation and interest rates are considered beyond the scope of this work and are therefore excluded.

2.2.2. Storage investment

Following the approach from [48,49], the investment cost of the utility-scale ESS is calculated considering three cost terms: initial investment (I_s^0), energy rating (I_s^E), and power rating (I_s^Q). I_s^0 represents the upfront capital required to cover expenses like site preparation, equipment procurement, labour costs, engineering, permitting, and other associated costs. I_s^E refers to the cost for the energy components determining the amount of energy that the system can store. This term considers the cost per unit of energy, measured in €/MWh. It represents the cost of adding 1 MWh of energy storage capacity to the system and is primarily influenced by the cost of the battery modules or cells used. I_s^Q refers to the maximum power output that the storage can provide and is expressed as the cost per unit of power in €/MW. This cost refers to increasing the power output of the energy storage system by 1 MW. It takes into account factors such as power conversion equipment, balance of system components, and electrical infrastructure upgrades. Other cost factors, such as maintenance and battery degradation, are left for future research.

2.2.3. Power system modelling

Let us consider a power system as a directional graph with $\mathcal{N}$ nodes (i.e., buses) and $\mathcal{E}$ edges (i.e., connections). Index $n \in \mathcal{N}$ is used to refer to every node where $\mathcal{N}$ is the set of all nodes in the system. Operator $n(.)$ counts over the member of the set. Suppose that there is at least a flexible and/or an in-flexible producer ($g \in \mathcal{G}_n$) and a set of in-flexible consumers ($l \in \mathcal{L}_n$) at every node where $\mathcal{G}_n$ ($\mathcal{L}_n$) is the set of generators (consumers) in node n and $\mathcal{G}$ ($\mathcal{L}$) is the set of all generators (consumers). Subscripts g and l respectively correspond to generation and demand. In addition to conventional generators, we assume that there can be a set of wind generators $w \in \mathcal{W}_n \subseteq \mathcal{W}$ where $\mathcal{W}_n$ denotes the set of wind generators in node n and $\mathcal{W}$ is the set of all wind generators. In addition to the supply and demand units, there can be storage units $s \in \mathcal{S}_n \subseteq \mathcal{S}$ placed in the node where s counts over storage units and $\mathcal{S}_n$ is the set of all possible storage units that can be located at node n and $\mathcal{S}$ is the set of all possible storage units in the network. Tuple (n, m) refers to the line connecting node n to node m when power flows from n to m. Index $t \in \mathcal{T}$ refers to every instance in time and $\mathcal{T}$ is the set of all time instances. Index $i \in [D, R]$ is used to refer to the day-ahead (D) or the real-time (R) (i.e., ancillary service) market.

2.2.4. Uncertainty modelling

The model focuses on wind power generation as the sole source of uncertainty. The uncertainty associated with wind power is captured using a moment-based ambiguity set, which characterizes the uncertainty arising from forecast errors in DA wind power predictions. Inspired by previous studies [50,51], the model assumes that the errors in wind power forecasts follow an unknown multivariate probability distribution. To encompass the overall system uncertainty, a vector of random variables $\Delta = [\omega_{1,1}, \omega_{2,1}, \dots, \omega_{w,t}] \in \mathbb{R}^Z$ is defined, where w and t represent the specific space and time dimensions. Consequently, the moment-based ambiguity set encloses all possible probability distributions that share the same first and second-order moments, and it can be expressed as follows:

$$\Pi = \{\mathbb{P} \in \Pi_0(\mathbb{R}^Z) : \mathbb{E}_{\mathbb{P}}[\Delta] = \mu^{\Pi},\ \mathbb{E}_{\mathbb{P}}[\Delta\Delta^T] = \Sigma^{\Pi}\}.$$

This set, denoted as Π, contains all probability distributions described by known parameters: the mean (μ^{Π}) and covariance (Σ^{Π}) of the wind forecast errors. The expectation is denoted by $\mathbb{E}_{\mathbb{P}}$, and the transpose operator is represented by ^{T}. It is assumed that the mean is zero and the covariance matrix can be estimated from empirical data on wind forecast errors. The covariance matrix captures the spatial correlation between wind forecast errors at a specific time in its diagonal entries, while the off-diagonal entries describe the temporal dependence. The total deviation from the DA forecast of all wind farms at a given time is given by the dot product of the unit vector ϕ^T and the wind forecast error vector Δ_t. A non-negative value of $\phi^T\Delta_t$ indicates a shortage of wind power during RT operation compared to the DA point forecast.

In this study, we have chosen to adopt the moment-based DRCC approach for the following reasons. Firstly, unlike SBSO and chance-constrained optimization methods, the DRCC approach does not rely on assumptions about the underlying probability distribution. This is advantageous in our context, where errors from imperfect forecasting algorithms may not follow a specific distribution, as discussed in [50]. Secondly, the DRCC approach is more computationally efficient than SBSO and distance-based DRO, making it particularly suitable given the high-dimensional state space from a one-year simulation and the complex, temporally coupled decision-making process involved in detailed ESS order clearing. Lastly, it offers greater adaptability and is less conservative than traditional RO.

2.3. Mathematical formulation of the problem

In this section, we formulate the optimal energy storage investment and flexible unit participation in the DA and RT markets as a Distributionally Robust Chance-Constrained Program (DRCCP). In Section 2.3.1, we provide the general formulation of the proposed DRCCP. In Section 2.3.2, we explain the procedure for reformulating the probabilistic DRCC program as an equivalent deterministic SOCP. Finally, in Section 3, we present the complete and tractable problem for ESS storage investment and market participation, formulated as a MISOCP.

2.3.1. Generic DRCC problem

The uncertainty-aware energy storage investment and market participation problem, proposed here, is first introduced as a generic DRCC program in Eqs. (1a)–(1d). The objective function (1a) employs a min–max structure, aiming to minimize the social cost of the market while maximizing the worst-case expected cost due to wind power forecast errors observed in real time. This is modelled using the worst-case probability distribution, which is the probability distribution leading to the highest expected cost due to the worst-case uncertainty realization.

$$\underset{\tilde{\Xi},\mathbb{P}\in\Pi}{MinMax} \quad \mathbb{E}_{\mathbb{P}}\left[\sum_{t\in\mathcal{T}}\sum_{u\in\mathcal{U}} C(\tilde{q}_{u,t})\right] \tag{1a}$$

s.t.

$$X(\tilde{q}_{u,t}) = 0 \qquad u\in\mathcal{U}, t\in\mathcal{T} \tag{1b}$$

$$Y(\tilde{q}_{u,t}) \geq 0 \qquad u\in\mathcal{U}, t\in\mathcal{T} \tag{1c}$$

$$\underset{\mathbb{P}\in\Pi}{min}\mathbb{P}[\tilde{q}_{u,t} \leq \overline{Q}_u] \geq (1-\epsilon) \qquad u\in\mathcal{U}, t\in\mathcal{T} \tag{1d}$$

$\tilde{\Xi} := \{\tilde{q}_{u,t} | u \in \mathcal{U}, t \in \mathcal{T}\}$ is the set of optimization decision variables. The term $C(\tilde{q}_{u,t})$ in the objective function represents the adjusted net aggregated social costs of the market. This is defined as the sum of aggregated social costs and the cost of temporal and energy-to-flexibility arbitrage. This results in an optimization problem where the flexibility cost is externalized from the social cost, as further elaborated in Section 3. Constraints (1b) and (1c) represent generic deterministic equalities and inequalities. Variables $\tilde{q}_{u,t} \in \mathbb{R}$ represent generic power or energy components associated with the power system under study, where u is the specific unit (e.g., wind producer, thermal power generator, load, storage unit, etc.) and t is the time instance. Similarly, $\overline{Q}_u$ is a parameter representing the upper bound of the variable $\tilde{q}_{u,t}$ (e.g., maximum generator output). The symbol tilde (i.e., $\tilde{}$) indicates a stochastic process, which signifies that the decision variable comprises both its nominal and uncertainty-dependent components.

The inequalities (1d) are formulated as DRCCs. Each DRCC ensures fulfilling the underlying constraint with the confidence level of 1 - ϵ under the worst-case distribution $\mathbb{P}$. The violation probability ϵ is a non-negative parameter. In this study, we adopt the individual chance constraints formulation. This formulation provides the system operator with a degree of freedom to adjust the violation probability for each constraint separately. An alternative approach could be the utilization of a joint chance-constrained framework, where the overall system reliability is guaranteed with a high probability. In such a framework, the system operator assigns a single violation probability for the entire set of chance constraints.

Solving the DRCC program (1a)–(1d) presents substantial computational challenges due to its inherent complexity. DRCC optimization problems are inherently difficult to solve as they involve an unknown set of probability distributions, resulting in a potentially infinite number of variables and constraints. Despite this, computational tractability for DRCC problems can be achieved across various ambiguity sets by leveraging affine control policies, convex approximations, and duality theory for moment problems, as discussed in [52].

To improve the computational tractability of the DRCC program, we use affine decision rules to model flexible unit behaviour as linear functions of wind forecast errors. These rules act as control actions, managing system responses to uncertainty. We reformulate DRCCs as deterministic Second-Order Cone (SOC) constraints, based on a modified version of Chebyshev's Inequality as explained in [53]. Our choice of SOC reformulation aligns with [33,54]. We exclude improved approximations like those presented in [55] as they introduce higher levels of mathematical complexity and necessitate auxiliary decision variables. This could potentially impact the scalability and computational efficiency of the problem. Hence, these enhancements are left as future work. The reformulation procedure for the probabilistic DRCC problem is explained in Section 2.3.2.

2.3.2. Reformulation of DRCC problem

As outlined above, the DRCC program (1a)–(1d) is computationally intractable in its original form and requires reformulation for practical implementation. To address this, affine response policies are introduced to manage the flexibility of assets such as power generators and storage units within the electricity network during the DA stage. These policies allocate flexibility reserves in addition to the scheduled nominal DA plan, considering the worst-case expected uncertainty realization during the RT stage. A generic flexible unit u can adjust its production or consumption level in response to wind forecast errors. This is modelled as follows:

$$\tilde{q}_{u,t} = \hat{q}_{u,t} + (\phi^T \Delta_t)\breve{q}_{u,t} \quad u\in\mathcal{U}, t\in\mathcal{T}, \tag{2}$$

where $\tilde{q}_{u,t}$ represents the stochastic power or energy component of unit u at time t. It is comprised of two parts: the nominal component $\hat{q}_{u,t}$ (denoted by the symbol $\hat{}$) and the uncertainty-dependent component $\breve{q}_{u,t}$ (denoted by the symbol $\breve{}$). The component $\breve{q}_{u,t}$ is the uncertainty response factor which indicates the contribution of unit u towards compensating the total wind power mismatch $\phi^T \Delta_t$ at time t. A comparable methodology is employed to characterize the affine response to uncertainty for all stochastic decision variables.

Following the approach in [33], we define the term $(\phi^T \Delta_t)\breve{q}_{u,t} := (\breve{q}_{u,t})\mu_t + \sqrt{\frac{1-\epsilon}{\epsilon}}\,\|\breve{q}_{u,t}\Sigma_t^{1/2}\|_2$, where μ_t is the mean forecast error at time t and $\Sigma_t^{1/2}$ is the square root of the covariance matrix of wind forecast errors at time t. For brevity, we rewrite this as $(\breve{q}_{u,t})\mu_t + \epsilon'\gamma_t\breve{q}_{u,t}$, where $\epsilon' := \sqrt{\frac{1-\epsilon}{\epsilon}}$ and $\gamma_t\breve{q}_{u,t} := \|\breve{q}_{u,t}\Sigma_t^{1/2}\|_2$. Considering the incorporation of the affine response policy to address uncertainty as described in (2), and assuming a zero mean forecast error (i.e., $\mu_t = 0$), the DRCC (1d) can be approximated by the following deterministic SOC constraint:

$$\epsilon'\gamma_t\breve{q}_{u,t} \leq \overline{Q}_u - \hat{q}_{u,t} \quad u\in\mathcal{U}, t\in\mathcal{T}, \tag{3}$$

Constraint (3) ensures that the sum of nominal ($\hat{q}_{u,t}$) and uncertainty-dependent ($\epsilon'\gamma_t\breve{q}_{u,t}$) power (or energy) components stays within the predefined upper bound ($\overline{Q}_u$) with a confidence level of $1-\epsilon$. A similar approach is used to reformulate the DRCCs emerging in the complete ESS investment and market participation problem presented in Section 3. For a more detailed explanation of the DRCC reformulation procedure outlined above we refer to [32]. Finally, recall that the mean of the forecast error uncertainty vector is assumed to be zero (i.e., $\mu_t = 0$). Consequently, the expectation operator in the objective function (1a) can be omitted, simplifying it into a single minimization function. For a detailed explanation and mathematical proof, we refer the reader to [50,55].

3. Tractable problem formulation

In this section, we present the complete, tractable formulation of the uncertainty-aware energy storage investment and market participation problem. This formulation incorporates the proposed novel BOs, the modelling assumptions, and the DRCC reformulation introduced in Section 2.

3.1. Objective function

The objective function (4) aims to minimize the adjusted net aggregated social cost of the power system over a one-year simulation horizon considering hourly steps. This objective incorporates several key components representing different aspects of the power system scheduling, operation and flexibility procurement from generators and storage units. The primary components of the objective function are as follows: the aggregated social cost, the arbitrage cost of energy in the DA market, the cost of energy used for flexibility arbitrage from the DA to the RT market, and the costs associated with procuring flexibility

from generators and storage units. This translates into the objective function below:

$$\underset{\Xi,\mathbb{P}\in\Pi}{Min} \sum_{t\in\mathcal{T}} \left[\left(\sum_{g\in\mathcal{G}} \hat{q}^{G}_{g,t} p^{G}_{g,t} - \sum_{l\in\mathcal{L}} \hat{q}^{L}_{l,t} p^{L}_{l,t} + \sum_{s\in\mathcal{S}} p^{spr}_{s} \hat{q}^{ch,D}_{s,t} - \sum_{s\in\mathcal{S}} \tilde{\lambda}_t \hat{q}^{ch,D\to R}_{s,t} \right) + \sum_{g\in\mathcal{G}} C^{Av}_{g} \alpha_{g,t} + \sum_{s\in\mathcal{S}} C^{Av}_{s} \eta^{dc}_{s} \beta_{s,t} \right] \tag{4}$$

where $\Xi := \Xi_g \cup \Xi_f \cup \hat{\Xi}_s \cup \check{\Xi}_s$ is the set of optimization decision variables; $\Xi_g := \{ \hat{q}^{G}_{g,t}, \check{q}^{G}_{g,t}, \hat{q}^{L}_{l,t}, \hat{q}^{W}_{w,t}, \alpha_{g,t} \mid g \in \mathcal{G}\ l \in \mathcal{L},\ w \in \mathcal{W},\ t \in \mathcal{T} \}$; $\Xi_f := \{ \hat{f}_{n,m,t}, \check{f}_{n,m,t}, \hat{\theta}_{n,t}, \check{\theta}_{n,t} \mid n \in \mathcal{N},\ (n,m) \in \mathcal{E},\ t \in \mathcal{T} \}$; $\hat{\Xi}_s := \{ \hat{e}^{D}_{s,t}, \hat{e}^{D\to R}_{s,t}, \hat{q}^{ch}_{s,t}, \hat{q}^{ch,D}_{s,t}, \hat{q}^{ch,D\to R}_{s,t}, \hat{q}^{dc}_{s,t}, \overline{E}_s, \overline{Q}_s, U_s, \beta_{s,t} \mid s \in \mathcal{S},\ t \in \mathcal{T} \}$; $\check{\Xi}_s := \{ \check{e}_{s,t}, \check{q}^{ch}_{s,t}, \check{q}^{ch,D\to R}_{s,t}, \check{q}^{dc}_{s,t}, \check{q}_{s,t} \mid s \in \mathcal{S},\ t \in \mathcal{T} \}$.

The aggregated social cost is defined as the cost of production minus the benefit of consumption. Specifically, it is given by the difference between the generation cost, $\hat{q}^{G}_{g,t} p^{G}_{g,t}$, and the load cost, $\hat{q}^{L}_{l,t} p^{L}_{l,t}$, for each time period t. The generation cost refers to the cost of producing energy, while the load cost reflects the benefit associated with consuming energy. The price terms, $p^{G}_{g,t}$ and $p^{L}_{l,t}$, represent the marginal production cost of generator g and the estimated bid price for conventional load l, respectively, at time t.

In addition to the aggregated social cost, the objective function includes the arbitrage cost of energy in the DA market. This term, $p^{spr}_{s} \hat{q}^{ch,D}_{s,t}$, accounts for the cost associated with participating in DA market arbitrage. The parameter p^{spr}_{s} represents the price spread, which indicates the minimum price difference at which the ESS is willing to engage in DA market arbitrage. Furthermore, the objective includes the cost of energy flexibility arbitrage from the DA to the RT market, represented by the term $\tilde{\lambda}_t \hat{q}^{ch,D\to R}_{s,t}$. Here, $\tilde{\lambda}_t$ is the predicted market clearing price at time t, and $\hat{q}^{ch,D\to R}_{s,t}$ represents the amount of energy transferred for flexibility between the DA and RT markets. This term models the costs incurred when energy is moved from the DA market to the RT market in response to real-time wind power generation deviations.

Finally, the objective function accounts for the costs of procuring flexibility from both generators and storage units. The terms $C^{Av}_{g} \alpha_{g,t}$ and $C^{Av}_{s} \eta^{dc}_{s} \beta_{s,t}$ represent the flexibility procurement costs from flexible generators and storage units, respectively. The parameters C^{Av}_{g} and C^{Av}_{s} denote the energy-to-flexibility spreads for these units, which reflect the price at which they are willing to provide flexibility in the RT market. Parameter η^{dc}_{s} denotes the discharging efficiency of the ESS. This formulation leads to an augmented market clearing problem, where the flexibility procurement costs in the RT market are externalized from the DA social cost. By doing so, it captures the economic impact of flexibility procurement and arbitrage while maintaining consistency with market operations. It is important to note that wind power generation is assumed to have zero marginal production cost, represented by $\hat{q}^{W}_{w,t} = 0$ for all $w \in \mathcal{W}$. Therefore, it is excluded from the objective function.

3.2. DA power network constraints

Constraints (5a) through (5f) represent the nominal power network constraints associated with the DA market. These constraints ensure that power generation, consumption, and transmission are balanced within specified bounds, maintaining the integrity and feasibility of the DA market operation.

$$\underline{Q}^{L}_{l} \le \hat{q}^{L}_{l,t} \le \overline{Q}^{L}_{l} \qquad l \in \mathcal{L}, t \in \mathcal{T} \tag{5a}$$

$$\underline{Q}^{G}_{g} \le \hat{q}^{G}_{g,t} \le \overline{Q}^{G}_{g} \qquad g \in \mathcal{G}, t \in \mathcal{T} \tag{5b}$$

$$\underline{Q}^{W}_{w} \le \hat{q}^{W}_{w,t} \le \overline{Q}^{W}_{w} \qquad w \in \mathcal{W}, t \in \mathcal{T} \tag{5c}$$

$$\sum_{g\in G_n} \hat{q}^{G}_{e,t} + \sum_{w\in W_n} \hat{q}^{W}_{w,t} + \sum_{s\in S_n} \hat{q}^{dc}_{s,t} \eta^{dc}_{s} = \sum_{l\in L_n} \hat{q}^{L}_{l,t} + \sum_{s\in S_n} \hat{q}^{ch}_{s,t} + \sum_{m\in\Omega_n} \hat{f}_{n,m,t} \qquad n \in \mathcal{N}, t \in \mathcal{T} \tag{5d}$$

$$\hat{f}_{n,m,t} = B_{n,m}(\hat{\theta}_{n,t} - \hat{\theta}_{m,t}) \qquad n,m \in \mathcal{E}, t \in \mathcal{T} \tag{5e}$$

$$\hat{\theta}_{n,t} = 0, \qquad n = ref, t \in \mathcal{T} \tag{5f}$$

Constraint (5a) establishes load limits. It ensures that the electricity demand from loads ($\hat{q}^{L}_{l,t}$) is within specified lower ($\underline{Q}^{L}_{l}$) and upper ($\overline{Q}^{L}_{l}$) bounds for each load l and time t. Note that his study assumes the demand to be inelastic (i.e., $\underline{Q}^{L}_{l} = \overline{Q}^{L}_{l}$). However, this assumption can be relaxed without loss of generality in our model. Constraint (5b) sets conventional generator limits. It restricts the power produced by conventional generators ($\hat{q}^{G}_{g,t}$) between minimum ($\underline{Q}^{G}_{g}$) and maximum ($\overline{Q}^{G}_{g}$) capacities for each generator g and time t. Similarly, constraint (5c) defines wind generation limits. It ensures that wind power generation ($\hat{q}^{W}_{w,t}$) stays within lower ($\underline{Q}^{W}_{w}$) and upper ($\overline{Q}^{W}_{w}$) bounds for each wind generator w and time t. Eq. (5d) represents the power balance constraint. It ensures that at each bus n and time t, the sum of power from conventional generators, wind generators, and ESS discharging equals the sum of load demands, ESS charging, and net power outflows. The efficiency factors η^{dc}_{s} and η^{ch}_{s} account for energy losses during discharging and charging of ESS, respectively. Constraint (5e) defines power flow using DC power flow approximation. It calculates the power flow ($\hat{f}_{n,m,t}$) between buses n and m at time t based on the voltage angle difference and line susceptance ($B_{n,m}$). This approximation assumes that all bus voltage magnitudes are equal to 1 per unit (p.u.), and that voltage angle differences are small. Constraint (5f) sets the reference bus. It fixes the voltage angle ($\hat{\theta}_{n,t}$) at the reference bus to zero for all time periods.

3.3. RT power network constraints

Constraints (6a) through (6i) represent the uncertainty-dependent power network constraints associated with the RT market. These constraints ensure the safe and reliable operation of the power network in RT by accounting for adjustments in generation, storage (dis)charging operations, and power flows to accommodate the worst-case deviations in wind power generation.

$$\epsilon' \gamma_t \check{q}^{G}_{g,t} \le \overline{Q}^{G}_{g} - \hat{q}^{G}_{g,t} \qquad g \in \mathcal{G}, t \in \mathcal{T} \tag{6a}$$

$$\epsilon' \gamma_t \check{q}^{G}_{g,t} \ge \underline{Q}^{G}_{g} - \hat{q}^{G}_{g,t} \qquad g \in \mathcal{G}, t \in \mathcal{T} \tag{6b}$$

$$\sum_{g\in\mathcal{G}} \check{q}^{G}_{e,t} + \sum_{s\in\mathcal{S}} \check{q}^{dc}_{s,t} \eta^{dc}_{s} - \sum_{s\in\mathcal{S}} \check{q}^{ch}_{s,t} = 1 \qquad t \in \mathcal{T} \tag{6c}$$

$$\sum_{g\in G_n} \check{q}^{G}_{e,t} + \sum_{s\in S_n} \check{q}^{dc}_{s,t} \eta^{dc}_{s} = \sum_{s\in S_n} \check{q}^{ch}_{s,t} + \sum_{m\in\Omega n} \check{f}_{n,m,t} \qquad n \in \mathcal{N}, t \in \mathcal{T} \tag{6d}$$

$$\epsilon' \gamma_t \check{f}_{n,m,t} \le \overline{f}_{n,m} - \hat{f}_{n,m,t} \qquad n,m \in \mathcal{E}, t \in \mathcal{T} \tag{6e}$$

$$\epsilon' \gamma_t \check{f}_{n,m,t} \ge \underline{f}_{n,m} - \hat{f}_{n,m,t} \qquad n,m \in \mathcal{E}, t \in \mathcal{T} \tag{6f}$$

$$\check{f}_{n,m,t} = B_{n,m}(\check{\theta}_{n,t} - \check{\theta}_{m,t}) \qquad n,m \in \mathcal{E}, t \in \mathcal{T} \tag{6g}$$

$$\check{\theta}_{n,t} = 0 \qquad n = ref, t \in \mathcal{T} \tag{6h}$$

$$\alpha_{g,t} \ge \epsilon' \gamma_t \check{q}_{g,t} \qquad g \in \mathcal{G}, t \in \mathcal{T} \tag{6i}$$

Constraints (6a) and (6b) define the upper and lower bounds of power generation for flexible generators. They ensure that the sum of nominal power generation ($\hat{q}^{G}_{g,t}$) and uncertainty-dependent generation adjustments ($\epsilon' \gamma_t \check{q}^{G}_{g,t}$) remains within the operational limits defined by $\overline{Q}^{G}_{g}$ and $\underline{Q}^{G}_{g}$, respectively. Constraint (6c) specifies the total uncertainty-dependent response in the system. It ensures that the uncertainty-dependent adjustments from generators ($\check{q}^{G}_{g,t}$), storage discharging ($\check{q}^{dc}_{s,t}$), and storage charging ($\check{q}^{ch}_{s,t}$) collectively sum to 1, which represents

the normalized total wind power deviation. Constraint (6d) maintains power balance at each bus, ensuring that uncertainty-dependent adjustments from generation and storage match the adjustments required by power flows in connected transmission lines ($\check{f}_{n,m,t}$). Constraints (6e) and (6f) define the upper and lower bounds for the uncertainty-dependent power flows through transmission lines. These constraints ensure that the sum of nominal flows ($\hat{f}_{n,m,t}$) and uncertainty-dependent flow adjustments ($\epsilon' \gamma t \check{f}_{n,m,t}$) remains within the specified limits, $\overline{f}_{n,m}$ and $\underline{f}_{n,m}$. Constraint (6g) relates uncertainty-dependent power flows to voltage angle differences ($\check{\theta}_{n,t} - \check{\theta}_{m,t}$) across buses through the line susceptance $B_{n,m}$. This constraint represents the DC power flow approximation for the RT adjustments. Constraint (6h) sets the reference bus voltage angle in RT to zero. Finally, constraint (6i) relates the flexibility of generators in real units (i.e., MW), represented by the auxiliary variable $\alpha_{g,t}$, to the normalized uncertainty-dependent adjustment $\check{q}^G_{g,t}$. The right-hand side $\epsilon' \gamma_t \check{q}^G_{g,t}$ represents the actual flexibility required in response to wind power deviations, where $\epsilon' \gamma_t$ scales the normalized adjustment to real units. This constraint, though relaxed, becomes exact as the objective function minimizes $\alpha_{g,t}$, ensuring $\epsilon' \gamma_t \check{q}^G_{g,t} = \alpha_{g,t}$.

3.4. DA storage system constraints

Constraints (7a) to (7i) represent the nominal storage constraints in the DA market. These constraints model the ESS operations during the DA stage, ensuring that charging, discharging, and energy states are managed effectively while respecting the assigned energy and power ratings.

$$\hat{q}^{ch}_{s,t} = \hat{q}^{ch,D}_{s,t} + \hat{q}^{ch,D\to R}_{s,t} \qquad s \in \mathcal{S}, t \in \mathcal{T} \quad (7a)$$

$$0 \le \hat{q}^{ch}_{s,t} \le \overline{Q}_s \qquad s \in \mathcal{S}, t \in \mathcal{T} \quad (7b)$$

$$0 \le \hat{q}^{dc}_{s,t} \le \overline{Q}_s \qquad s \in \mathcal{S}, t \in \mathcal{T} \quad (7c)$$

$$\hat{e}^{D}_{s,t} = \hat{e}^{D}_{s,t-1} + \eta^{ch}_s \hat{q}^{ch,D}_{s,t} - \hat{q}^{dc}_{s,t} \qquad s \in \mathcal{S}, t \in \mathcal{T} \quad (7d)$$

$$\hat{e}^{D\to R}_{s,t} = \hat{e}^{D\to R}_{s,t-1} + \eta^{ch}_s \hat{q}^{ch,D\to R}_{s,t} - \beta_{s,t} \qquad s \in \mathcal{S}, t \in \mathcal{T} \quad (7e)$$

$$\hat{e}^{D}_{s,t} = e^0_s \qquad s \in \mathcal{S}, t \in \mathcal{T}^{24} \quad (7f)$$

$$\hat{e}^{D\to R}_{s,t} = e^0_s \qquad s \in \mathcal{S}, t \in \mathcal{T}^{24} \quad (7g)$$

$$0 \le \hat{e}^{D}_{s,t} + \hat{e}^{D\to R}_{s,t} \le \overline{E}_s \qquad s \in \mathcal{S}, t \in \mathcal{T} \quad (7h)$$

$$\hat{e}^{D}_{s,t} + \eta^{ch}_s \hat{q}^{ch,D\to R}_{s,t} \le \overline{E}_s \qquad s \in \mathcal{S}, t \in \mathcal{T} \quad (7i)$$

Constraint (7a) defines the total energy charged by the ESS, $\hat{q}^{ch}_{s,t}$, as the sum of the energy charged for the DA market, $\hat{q}^{ch,D}_{s,t}$, and the portion reserved for flexibility services in the RT market, $\hat{q}^{ch,D\to R}_{s,t}$. Constraints (7b) and (7c) ensure that the charging and discharging powers, respectively, remain within the maximum power rating, $\overline{Q}_s$, for all periods. Note that $\overline{Q}_s$ is a decision variable in our problem. Constraint (7d) represents the energy balance for the DA market. It ensures that the energy stored at time t, $\hat{e}^{D}_{s,t}$, equals the previous energy state at time $t-1$ plus the energy charged, $\eta^{ch}_s \hat{q}^{ch,D}_{s,t}$, minus the energy discharged, $\hat{q}^{dc}_{s,t}$. Constraint (7e) ensures energy balance for the portion of storage capacity reserved for cross-market arbitrage. $\hat{e}^{D\to R}_{s,t}$ is updated based on the charging in the DA market for the RT market and the discharging in the RT market, denoted by $\beta_{s,t}$. Constraints (7f) and (7g) require that the state of energy in both the DA and RT markets returns to the initial value, e^0_s, at the end of the day (i.e., $t \in \mathcal{T}^{24}$). This ensures the closure of the daily cycle and maintains consistency with the DA market structure. Constraint (7h) ensures that the combined energy state for both markets remains within the storage's maximum energy rating, $\overline{E}_s$, which is also treated as a decision variable. Finally, constraint (7i) limits cross-market arbitrage by ensuring that the energy charged in the DA market for the RT market, $\hat{q}^{ch,D\to R}_{s,t}$, respects the available storage capacity. This constraint prevents situations where the ESS commits to charging more than its available capacity in the DA market for the RT market, by exploiting its ability to reduce the charging amount in the RT market. The role of this constraint is to enforce the non-anticipativity conditions and effectively prevent overcharging scenarios in DA for the RT market.

3.5. RT storage system constraints

Constraints (8a) to (8j) represent the uncertainty-dependent storage constraints in the RT market. They model the uncertainty-dependent behaviour of the ESS in the RT market by taking into account the changes in charging and discharging operations of the ESS in response to uncertainty in wind power generation.

$$\check{e}_{s,t} = \check{e}_{s,t-1} + \eta^{ch}_s \check{q}^{ch,D\to R}_{s,t} + \eta^{ch}_s \check{q}^{ch}_{s,t} - \check{q}^{dc}_{s,t} \qquad s \in \mathcal{S}, t \in \mathcal{T} \quad (8a)$$

$$\check{e}_{s,t} = e^0_s \qquad s \in \mathcal{S}, t \in \mathcal{T}^{24} \quad (8b)$$

$$0 \le \epsilon^{'} \gamma_t \check{e}_{s,t} \le \overline{E}_s - \hat{e}^{D}_{s,t} \qquad s \in \mathcal{S}, t \in \mathcal{T} \quad (8c)$$

$$0 \le \epsilon^{'} \gamma_t (\check{q}^{ch}_{s,t} + \check{q}^{ch,D\to R}_{s,t}) \le \overline{Q}_s - \hat{q}^{ch,D}_{s,t} \qquad s \in \mathcal{S}, t \in \mathcal{T} \quad (8d)$$

$$0 \le \epsilon^{'} \gamma_t \check{q}^{ch,D\to R}_{s,t} \le \hat{q}^{ch,D\to R}_{s,t} \qquad s \in \mathcal{S}, t \in \mathcal{T} \quad (8e)$$

$$0 \le \epsilon^{'} \gamma_t \check{q}^{dc}_{s,t} \le \overline{Q}_s - \hat{q}^{dc}_{s,t} \qquad s \in \mathcal{S}, t \in \mathcal{T} \quad (8f)$$

$$\beta_{s,t} \ge \epsilon^{'} \gamma_t \check{q}_{s,t} \qquad s \in \mathcal{S}, t \in \mathcal{T} \quad (8g)$$

$$\check{q}_{s,t} = \check{q}^{dc}_{s,t} - \check{q}^{ch}_{s,t} \qquad s \in \mathcal{S}, t \in \mathcal{T} \quad (8h)$$

$$\check{q}^{ch}_{s,t} = 0 \qquad s \in \mathcal{S}, t \in \mathcal{T} \quad (8i)$$

$$\sum_{g \in G} \alpha_{g,t} + \sum_{s \in S} \eta^{dc}_s \beta_{s,t} \le \epsilon^{'} \gamma_t \qquad t \in \mathcal{T} \quad (8j)$$

Eq. (8a) ensures the uncertainty-dependent state of energy at time t ($\check{e}_{s,t}$) equals the previous state plus the charging factor from DA to RT ($\check{q}^{ch,D\to R}_{s,t}$), RT charging ($\check{q}^{ch}_{s,t}$), minus RT discharging ($\check{q}^{dc}_{s,t}$). This equation reflects how the ESS responds to charging and discharging actions, accounting for the uncertainty in the RT market. Eq. (8b) ensures the uncertainty-dependent state of energy at the end of each day (i.e., $t \in \mathcal{T}^{24}$) matches the initial state, effectively closing the energy cycle for the day. Constraint (8c) ensures that the combined energy state, including the nominal energy state ($\hat{e}^{D}_{s,t}$) and the uncertainty-dependent energy state ($\epsilon' \gamma_t \check{e}_{s,t}$), does not exceed the storage's maximum capacity ($\overline{E}_s$). This enforces the capacity limit of the storage system in the real-time market. Constraint (8d) enforces that the sum of nominal and uncertainty-dependent charging rates ($\hat{q}^{ch}_{s,t}$ and $\check{q}^{ch,D\to R}_{s,t}$) remains within the maximum power rating of the ESS ($\overline{Q}_s$), ensuring that the storage system operates within its power limits. Constraint (8e) ensures that the uncertainty-dependent charging factor ($\check{q}^{ch,D\to R}_{s,t}$) remains between zero and the DA to RT charging rate ($\hat{q}^{ch,D\to R}_{s,t}$), enforcing the limits on cross-market charging. Constraint (8f) enforces the RT discharging capacity limit by ensuring that the uncertainty-dependent discharging rate ($\check{q}^{dc}_{s,t}$) stays within the storage's power rating. Constraint (8g) sets an upper bound on the flexibility offered by the ESS in the RT market, denoted by $\beta_{s,t}$. The relaxed form of this constraint ensures that the flexibility provided by the ESS in the RT market is bounded by the uncertainty-related term $\epsilon' \gamma_t \check{q}_{s,t}$. Since the objective function minimizes $\beta_{s,t}$, this relaxed constraint holds exactly, meaning $\epsilon' \gamma_t \check{q}_{s,t} = \beta_{s,t}$. Eq. (8h) defines the net uncertainty-dependent power rate of the ESS as the difference between the discharging rate ($\check{q}^{dc}_{s,t}$) and the charging rate ($\check{q}^{ch}_{s,t}$). Eq. (8i) ensures that the uncertainty-dependent charging rate ($\check{q}^{ch}_{s,t}$) in the RT market is zero. This constraint implies that no additional charging is permitted in the RT market beyond what was scheduled in the DA market. Finally, Eq. (8j) ensures that the total flexibility provided by both generators ($\alpha_{g,t}$) and storage units ($\eta^{dc}_s \beta_{s,t}$) does not exceed the worst-case wind power deviation, represented by the uncertainty term $\epsilon' \gamma_t$. This constraint guarantees that the total flexibility provided matches the maximum expected fluctuation in wind generation, ensuring balance and stability in the power system.

3.6. Storage investment constraints

Constraints (9a) through (9e) model the investment decisions for the ESS. They ensure that the power and energy ratings of the ESS meet operational requirements, while also making the ESS investment financially viable. This is achieved by balancing the ESS capital expenditure against returns from DA market arbitrage and RT market flexibility services.

$$\sum_{t\in\mathcal{T}}(p_s^{spr}\hat{q}_{s,t}^{ch,D}+C_s^{Av}\beta_{s,t})\le U_s I_s^0+I_s^E\overline{E}_s+I_s^Q\overline{Q}_s \qquad s\in\mathcal{S} \quad (9a)$$

$$\sum_{t\in\mathcal{T}}(\tilde{\lambda}_t\hat{q}_{s,t}^{dc}-\tilde{\lambda}_t\hat{q}_{s,t}^{ch,D}+C_s^{Av}\beta_{s,t})\ge U_s I_s^0+I_s^E\overline{E}_s+I_s^Q\overline{Q}_s \qquad s\in\mathcal{S} \quad (9b)$$

$$0\le\overline{E}_s\le U_s M \qquad s\in\mathcal{S} \quad (9c)$$

$$0\le\overline{Q}_s\le U_s M \qquad s\in\mathcal{S} \quad (9d)$$

$$\overline{Q}_s\eta_s^{ch}\le\overline{E}_s \qquad s\in\mathcal{S} \quad (9e)$$

Constraints (9a) and (9b) ensure that the ESS is only deployed if it can generate sufficient revenue to cover its investment costs, represented by the right-hand side of these constraints. The total investment cost includes the initial investment (I_s^0) as well as the costs for energy capacity ($I_s^E\overline{E}_s$) and power capacity ($I_s^Q\overline{Q}_s$). Specifically, constraint (9a) sets a lower bound for the ESS investment cost. It requires that the total investment cost be at least as large as the sum of the minimum revenue from DA market arbitrage ($p_s^{spr}\hat{q}_{s,t}^{ch,D}$), based on the price spread, and the revenue from RT market flexibility services ($C_s^{Av}\beta_{s,t}$). Constraint (9b) sets an upper bound for the ESS investment cost. It ensures that the total investment cost does not exceed the expected revenue, which is defined as the difference between ESS discharging revenue and charging cost (based on the DA price forecast, $\tilde{\lambda}_t$) plus the revenue from RT flexibility services ($C_s^{Av}\beta_{s,t}$). Constraints (9c) and (9d) determine whether the ESS should be deployed, with U_s serving as a binary decision variable. If the model opts to invest in storage ($U_s = 1$), the energy rating $\overline{E}_s$ and power rating $\overline{Q}_s$ are activated, allowing them to take values up to a sufficiently large constant M. Conversely, if $U_s = 0$, both ratings are set to zero, indicating that no ESS is deployed at that location. Finally, constraint (9e) ensures that the energy rating of the ESS is sufficiently large to handle the maximum power rating multiplied by the charging efficiency, η_s^{ch}. This guarantees that the storage system can fully utilize its power rating for at least one hour of operation.

3.7. Complete problem

Considering the variables and constraints previously described, the complete uncertainty-aware ESS investment and market participation problem (10) takes the following form:

$$\begin{aligned}
&\text{Minimize:} && (4)\\
&\text{s.t.}\\
&\text{DA Power Network Constraints:} && (5a)-(5f)\\
&\text{RT Power Network Constraints:} && (6a)-(6i)\\
&\text{DA Storage System Constraints:} && (7a)-(7i)\\
&\text{RT Storage System Constraints:} && (8a)-(8j)\\
&\text{Storage Investment Constraints:} && (9a)-(9e)
\end{aligned} \qquad (10)$$

The inequalities (6a), (6b), (6e), (6f), (6i), (8c), (8d), (8e), (8f) and (8g) are formulated as DRCCs. This formulation ensures that at the optimal solution, the probability of satisfying each constraint is modelled with a violation probability of no more than ϵ, or equivalently, a confidence level of at least (1 - ϵ). Note that ϵ can take different values for the individual chance constraints. The resulting DRCC problem (10) is a MISOCP that can be efficiently solved with off-the-shelf optimization solvers such as Mosek and Gurobi.

4. Results and discussion

4.1. Case study

The power transmission network utilized in this research is obtained by adapting the IEEE 24-Bus Reliability Test System [56]. The power network consists of 12 conventional generators, 2 wind farms with a maximum capacity of 500 MW each, 17 loads, and 2 potential storage units requiring investment decisions situated at buses 5 and 7. The different buses are connected with a set of 34 power transmission lines. The assumed initial cost (I_s^0) for installing the utility-scale ESS is 100,000 €. The cost per unit of energy (I_s^E) is 200,000 €/MWh. The cost per unit of power (I_s^Q) is set at 200,000 €/MW. The price spread (p^{spr}) is fixed at 4 €/MWh. The average lifetime of the ESS is 10 years. The storage investment costs are obtained from [49]. The energy-to-flexibility spread is set to 10 €/MW for both flexible generators (C_g^{Av}) and storage units (C_s^{Av}). The data on power network parameters, asset characteristics, and wind uncertainty modelling are available in the online appendix [57].

The selected period for the simulation is one year with a time resolution of one hour. The DA market-clearing price forecast $\tilde{\lambda}_t$ is based on historical data for the Netherlands obtained from [58] for the year 2022. To estimate the covariance matrix of wind forecast errors, a set of 1000 wind forecast scenarios is used for each day of the year, based on empirical data for the Netherlands obtained from [59]. The violation probability level (ϵ) is set to 0.1 for DRCCs (6a), (6b), (6e) and (6f), concerning the power network, and to 0.2 for DRCCs (8c), (8d), (8e) and (8f), concerning the storage system. It is important to note that ϵ is set to 0.5 for constraints (6i), (8g) and (8j). These constraints are used to map RT variables, expressed as a function of wind power deviation, back to DA units (i.e., MW). We choose to set ϵ to 0.5 in these constraints to prevent worst-case uncertainty back-propagation from RT to DA units. Note that when ϵ is set to 0.5, ϵ' is equal to 1. This implies that $\epsilon'\gamma_t = \|\Sigma_t^{1/2}\|_2$. This approach guarantees a resilient solution for the power network while preventing excessive conservatism in flexibility policies and storage investment decisions.

4.2. Numerical results

The problem is implemented in Julia v1.6.7, utilizing JuMP v1.14.1 and Mosek v9.3.22. The problem is solved using a laptop equipped with 32 GB RAM and an Intel(R) Xeon(R) processor with 6 cores running at 2.80 GHz. The average solution time is approximately one hour. The solution to the problem provides the nominal DA schedule, uncertainty-dependent decisions that account for variability in wind power generation in RT, and investment decisions related to the installation of the storage system.

4.2.1. Economic analysis and investment recovery

Table 1 presents the optimal energy storage investment decision. The results indicate that the optimal choice is to build a single utility-scale ESS located at bus 5 (denoted as S1). This storage system has an energy rating of 145.98 MWh and a power rating of 160.41 MW. In line with the problem formulation, we observe that the power rating is affected by charging and discharging efficiencies, set at 0.91 and 0.89 respectively. Considering the efficiency losses, the energy-to-power ratio of the storage system is approximately 1:1. The total investment for S1 is 61.4 M€. The storage system is expected to recover its investment over a 10-year lifetime with zero interest, resulting in an annualized capital cost of 6.14 M€/year. Notably, the ESS located at bus 7 (denoted as S2) was not selected for investment in the current setting. Since both storage systems have identical cost parameters, the results suggest that the decision is driven by the specific location of the ESS. The location of S1 in the network makes it a more suitable option compared to S2, considering the distribution of loads, generation, and

Table 1
Optimal energy storage investment decision. S1 and S2 represent storage units located at buses 5 and 7, respectively.

Metric	S1	S2	Unit
Energy rating	145.98	0.00	MWh
Power rating	160.41	0.00	MW
Total investment	$6.14 \cdot 10^7$	0.00	€

Table 2
Economic performance metrics at system, generator, and storage levels.

Level	Metric	Value	Unit
System	Utility	$6.21 \cdot 10^9$	€/year
	Social welfare DA	$6.22 \cdot 10^9$	€/year
	Flexibility cost RT	$7.40 \cdot 10^6$	€/year
Generators	Revenue DA	$4.65 \cdot 10^9$	€/year
	Revenue RT	$2.31 \cdot 10^6$	€/year
Storage	Revenue DA	$1.04 \cdot 10^6$	€/year
	Revenue RT	$5.10 \cdot 10^6$	€/year

transmission line limits. These results highlight the critical role of network constraints in determining the optimal location for ESS.

Next, we analyse the system's economic performance metrics, as presented in Table 2. The total system utility amounts to 6.21 B€/year, with the majority coming from DA social welfare, which is 6.22 B€/year. In contrast, the cost of procuring RT flexibility is much smaller, at 7.40 M€/year. Conventional generators obtain most of their revenue from DA power dispatch, amounting to 4.65 B€/year, while RT revenue is significantly lower, at 2.31 M€/year. For the storage system, Table 2 shows that revenue from DA arbitrage is 1.04 M€/year, while RT arbitrage generates a higher revenue of 5.10 M€/year. These revenues demonstrate the dual role of the storage system in contributing to both DA and RT market operations. Importantly, the total revenue from the storage system matches its annualized capital cost of 6.14 M€/year, ensuring investment recovery. Most of this recovery comes from RT arbitrage (83.1%), with DA arbitrage contributing a smaller but significant portion (16.9%). These findings underscore the effectiveness of the proposed DBOs and FBOs in facilitating ESS investment recovery. They also highlight the importance of both DA and RT arbitrage revenues in ensuring the financial viability of ESS, with the RT market playing a particularly critical role. The results demonstrate that the proposed methodology enables ESS to capitalize on revenue opportunities across multiple market segments, ensuring the recovery of ESS investments.

4.2.2. Day-ahead dispatch

To illustrate the working principle of our model, we focus on a representative operational day. Fig. 3 shows the daily aggregated DA schedule for the system. The load varies throughout the day between a minimum of about 2.2 GW and a maximum of 3.1 GW, following a typical duck curve. We note that conventional generators contribute significantly to the total power supply at all times, as shown by the grey area. Wind production, depicted in green, is higher between hours 1–8 and relatively lower afterwards. The storage system charges between hours 4–7, during the low demand period indicated by the red area, and discharges during peak demand at hour 10 as well as between hours 18–20, as indicated by the orange area. Additionally, the storage system charges a significant amount of energy for RT market arbitrage at all times, as shown by the black dotted area. Hourly Market Clearing Prices (MCPs) are generally high, ranging between 470–550 €/MWh. However, the absolute price difference of 80 €/MWh is comparable to other days of the year. MCPs are derived from the dual variable of the power balance constraint (5c). It must be noted that since our model is a mixed-integer problem, it does not directly yield MCPs. Therefore, a two-step simulation process is conducted. Firstly,the full simulation is executed. Secondly, the model is run with fixed binaries (i.e., U_s is fixed) to retrieve the MCPs.

4.2.3. Block order analysis

Fig. 4 illustrates the detailed ESS charging and discharging operations, along with the associated state of energy of the ESS associated with the DA and RT markets. During hours 1–2, the state of energy in the DA market ($\hat{e}^D$), depicted by the blue line, is nearly zero. It gradually increases between hours 3–7 due to DA charging events ($\hat{q}^{ch,D}$), reaching 115 MWh. This stored energy is then discharged at hours 10 and 18–20 ($\hat{q}^{dc}$) through temporal DA arbitrage, indicating that DBO had been accepted at those hours. Furthermore, the storage system consistently engages in RT temporal and energy-to-flexibility arbitrage throughout the day (i.e., FBO). Notably, the ESS charging rate from DA to RT ($\eta_s^{ch}\hat{q}^{ch,D\to R}$) is larger than the discharging rate in RT (β) at hours 1, 2, 4, 6, 7, and 10, as well as hours 15–16 and 18. Under these conditions, β represents a virtual discharging event (or a reduced scheduled charging rate), indicating that an FBO$^-$ type block order had been accepted at these hours. Simultaneously, part of the energy may still be charged, leading to an increase in the energy state of the battery reserved for RT flexibility services ($\hat{e}^{D\to R}$), depicted by the green line. The charged energy is then discharged in RT at hours 3, 5, 8, 11–14, and 21–24, resulting in a decrease in the state of energy of the ESS, which indicates that an FBO$^+$ type block order had been accepted at those hours. Furthermore, we note that FBO$^+$ is mostly accepted alongside FBO$^-$, meaning that flexibility can be delivered through a combination of reducing the charging rate and discharging previously accumulated energy in RT. Hour 5 stands out as the only time when the flexibility mechanism is solely FBO$^+$, indicating that the only available flexibility source in RT is the discharge of previously accumulated energy. These findings underscore the effectiveness of the proposed DBOs, FBOs and their combination in enhancing flexibility within the power system.

4.2.4. Flexibility reserves allocation

Fig. 5 shows the flexibility reserves provided by flexible generators (blue) and storage (orange). The bars represent the amount of flexibility contributed by each asset. Generation reserves signify increased power production, while storage reserves represent the flexibility obtained through FBOs. The combined flexibility from generators and storage must always equal the total expected wind power deviation, indicated by the green line. In this study, we consider a 50% probability (with $\gamma = \epsilon'$ and $\epsilon = 0.5$) as the most likely wind power deviation. Thus, the system is scheduled according to the orange and blue bars, representing the aggregated flexibility from storage and generators respectively. The results indicate that both generators and storage provide comparable flexibility during hours 1–10, when the wind deficit is most severe, peaking at 125 MW at hour 5. In contrast, between hours 11–24, the storage predominantly compensates for the wind power deficit. Furthermore, recall that DRCCs ensure that adequate capacity is left available for flexible units to accommodate worst-case wind deviations with a predefined confidence level, determined by the chosen value of ϵ. The red and grey bars illustrate the maximum capacity that can be offered by storage units and generators under the worst-case scenario considering the specified values of ϵ (i.e., 0.1 for generators and 0.2 for storage). The results indicate that the system maintains sufficient capacity to manage worst-case wind deficits at all times with a violation probability level of 0.2, as indicated by the orange line. Notably, as the violation probability level is further reduced to 0.1, depicted by the black line, the worst-case wind deviation increases and the system becomes unable to address the imbalances. This aligns with the assumptions made regarding the choice of ϵ for individual chance constraints. To ensure a higher confidence level in mitigating worst-case wind deviations, the system operator should opt for smaller values of ϵ. However, this may lead to a more conservative solution.

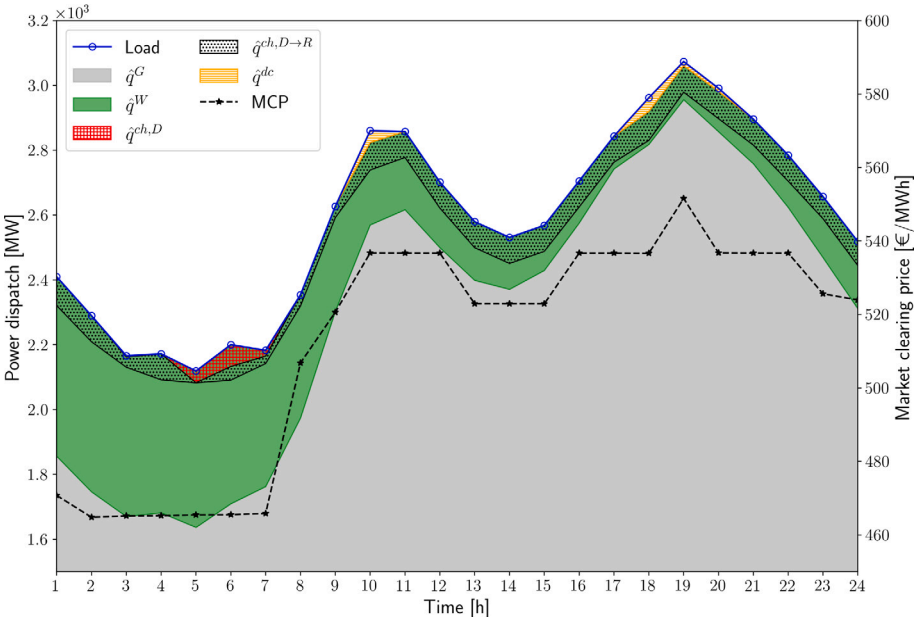

Fig. 3. DA schedule: total load (blue line), conventional generators (grey area), wind point forecast (green area), storage charging (red) and discharging (yellow) for DA arbitrage, charging for RT arbitrage (dotted area), and market clearing prices (black dashed line). (For interpretation of the references to colour in this figure legend, the reader is referred to the web version of this article.)

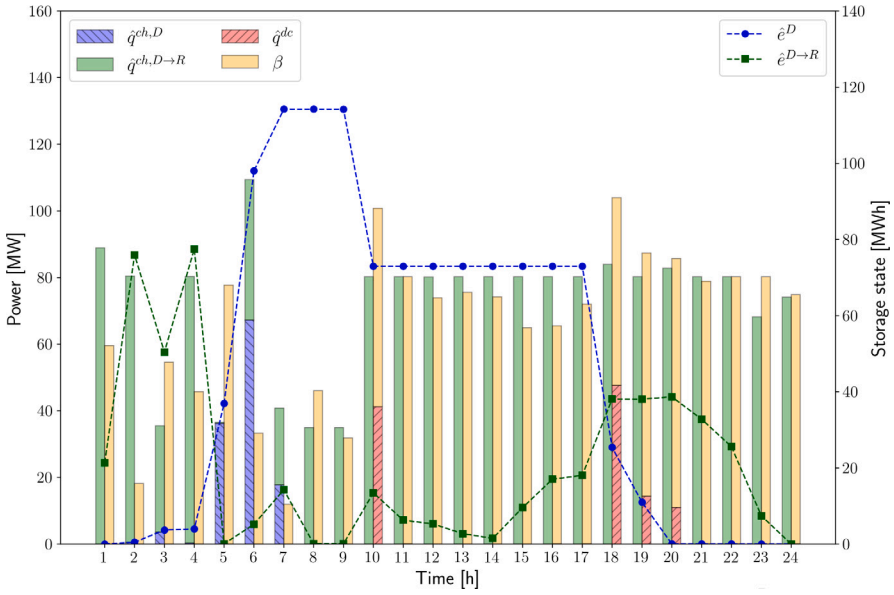

Fig. 4. Charging and discharging operations and state of energy of the ESS for DA (^{D}) and DA to RT ($^{D\to R}$) market segments. β indicates discharging in RT.

4.2.5. Annual charging and discharging frequency

The histograms in Fig. 6 depict the frequency of charging and discharging events in DA and RT (y-axis) and their respective magnitude ranges in MW (x-axis) over the entire year of simulation. Notably, the frequency of DA charging/discharging events is relatively lower compared to RT operations, in line with the lower DA revenue compared to RT revenue as observed in Table 2. The frequency of charging events decreases as the magnitude increases, while the frequency of discharging is higher in the 0–20 MW range, as well as in the 70–80 MW range and the 140–150 MW range. This indicates that discharging occurs more frequently in single large events as opposed to charging. Additionally, we note that the frequency of both charging and discharging events in RT increases with magnitude, approaching 4000 charging occurrences and 2800 discharging occurrences in the 80–90 MW range. Moreover, beyond the 80–90 MW range, no RT occurrences are observed, demonstrating the cumulative impact of considering the worst-case wind generation deviation throughout the year. Individual chance constraints ensure that the storage response does not exceed a designated maximum safety limit, taking into account the maximum installed capacity. Consequently, the storage system will never charge or discharge at its maximum capacity, as additional capacity must be reserved to respond to more challenging and unforeseen conditions. While this safety limit may reduce ESS revenue, it also ensures system reliability under unforeseen circumstances.

4.2.6. Impact of FBOs over the year

The box plot in Fig. 7 illustrates the share of storage flexibility as a percentage of the total wind power mismatch for each hour of the day, segmented by cross-market energy-to-flexibility FBO^{+} and FBO^{-}.

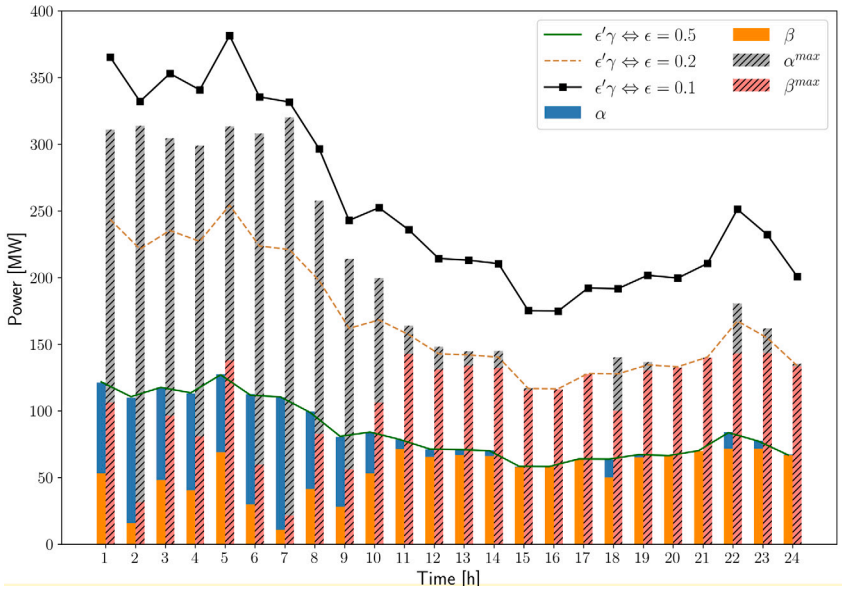

Fig. 5. Allocation of flexibility reserves: flexible generators (blue), flexible generators worst-case (grey), storage (orange), and storage worst-case (red). Green, orange and black lines represent the worst-case wind deviation in RT under different ϵ. (For interpretation of the references to colour in this figure legend, the reader is referred to the web version of this article.)

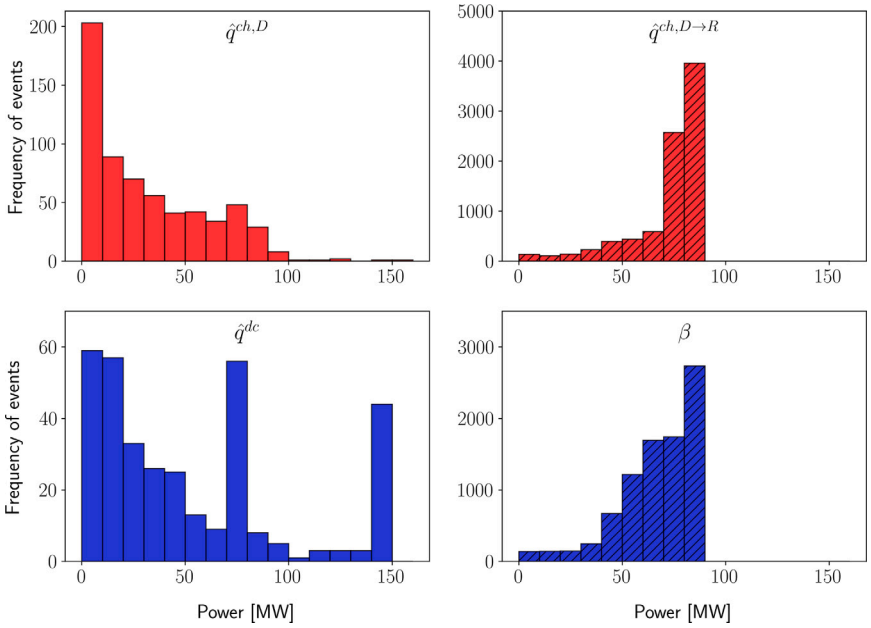

Fig. 6. Histogram showing the frequency of charging and discharging events in DA and RT (y-axis) and their magnitude (x-axis) for the whole year.

The light blue boxes represent FBO$^+$, indicating intertemporal arbitrage, while the green boxes represent FBO$^-$, indicating cross-market arbitrage within a single time instance. The boxes capture the middle 50% of the data (25th to 75th percentiles). The whiskers extend to the 10th and 90th percentiles, providing a sense of the data distribution and variability.

Results show that the distribution and variability of storage flexibility shares differ significantly between FBO$^+$ and FBO$^-$. The green boxes for FBO$^-$ indicate higher percentages and greater variability, with shares often exceeding 90%. In contrast, the light blue boxes for FBO$^+$ display lower values and less variability, suggesting that intertemporal energy-to-flexibility arbitrage is relatively less common and less substantial. The share of storage flexibility for FBO$^+$ typically remains below 20%, with some hours showing shares close to zero. Hours 4, 5, 14, and 23 are notable exceptions, with higher shares of flexibility from FBO$^+$ reaching above 20% and some extreme occurrences approaching up to 80%, as indicated by the whiskers. The red lines within the boxes indicate the median values. For FBO$^-$, the median values are consistently high, reaching levels between 60%–85%. In contrast, median values for FBO$^+$ remain significantly lower, often below 10%. Bear in mind that a large gap between the mean and median is an indication of the existence of outliers, which can significantly skew the data distribution and affect the overall analysis. The black triangles represent the mean values for each hour. In FBO$^+$, the means generally exceed the medians and are more widely spread, indicating a right-skewed distribution with occasional high values pulling the mean upwards. Conversely, in FBO$^-$, the means are generally lower and closer to the medians, suggesting fewer outliers

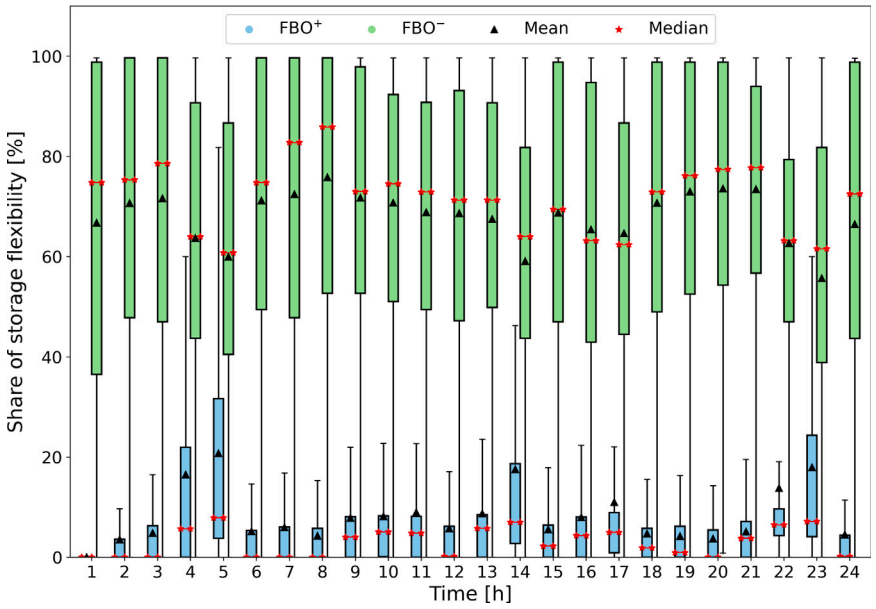

Fig. 7. Box plot illustrating the distribution of percentage share contributions of FBO$^+$ and FBO$^-$ in compensating the total wind power mismatch, derived from annual data displayed for 24 h.

in revenues. This also shows a slight left skewness due to occasional lower values pulling the mean downwards. Results indicate that the storage system is more actively involved in single-time cross-market arbitrage (FBO$^-$). In contrast, inter-temporal arbitrage in the RT market (FBO$^+$) is relatively less frequent but still significant. This reaffirms the effectiveness of the proposed FBOs in enabling ESS to capitalize on revenue opportunities in the RT market while effectively managing power imbalances throughout the year.

4.3. Sensitivity analysis

A one-factor-at-a-time sensitivity analysis is conducted to gain deeper insight into the model's behaviour under different hyperparameter settings. We examine the influence of varying constraint violation probability levels (ϵ) and energy-to-flexibility spreads (C_g^{Av} and C_s^{Av}) on the investment and operational strategy of the ESS. By varying ϵ, we demonstrate the impact of different levels of conservativeness in the individual chance constraints. Higher (lower) conservativeness in this context reflects the system's ability to respond to more (less) challenging conditions concerning wind power generation deviations in RT. On the other hand, varying the energy-to-flexibility spreads reflects the impact of different market conditions on optimal investment and operational decisions.

4.3.1. Constraint violation probability

Fig. 8 shows the impact of varying the constraint violation probability ϵ on storage revenue from both DBO (top) and FBO (bottom). A higher (lower) ϵ value implies a higher (lower) level of conservativeness of the solution. The violation probability level is varied between 0.1 and 0.4 for the DRCCs (6a), (6b), (6e), and (6f) concerning the power network denoted by ϵ_p (or just p), and for the DRCCs (8c), (8d), (8e), and (8f) concerning the storage system denoted by ϵ_s (or just s). The top chart of Fig. 8 illustrates the storage revenue from DBO for various combinations of ϵ values. The baseline scenario refers to the parameter settings used in the main case study.

For $\epsilon_s = 0.1$, storage revenue is zero across all ϵ_p values, indicating that ESS investment is not viable. For all other ϵ_s values, positive storage revenues are observed, indicating feasible ESS investments. The baseline scenario yields a storage revenue of 1.04 M€/year, which decreases as ϵ_s increases. For instance, with $\epsilon_p = 0.1$, revenue declines from 1.04 M€/year at $\epsilon_s = 0.2$ to 0.86 M€/year at $\epsilon_s = 0.4$. This decreasing trend persists for higher ϵ_p values, suggesting that more conservative solutions on the storage system constraints (lower ϵ_s) yield higher revenues from executing DBOs in the DA market.

The bottom chart of Fig. 8 shows storage revenue from FBO$^+$ and FBO$^-$ under various ϵ combinations. Similar to DBO revenue, when $\epsilon_s = 0.1$, FBO revenue is zero across all ϵ_p values, indicating unprofitable scenarios. In all profitable scenarios, FBO$^+$ revenue consistently contributes less than FBO$^-$ to the total revenue, ranging from about 10% at $\epsilon_s = 0.2$ to 20% at $\epsilon_s = 0.4$. Additionally, as ϵ_s increases, the total FBO revenue rises. For example, considering the scenarios with $\epsilon_p = 0.1$, the FBO revenue increases from 5.10 M€/year at $\epsilon_s = 0.2$ to 5.48 M€/year at $\epsilon_s = 0.3$ and 5.45 M€/year at $\epsilon_s = 0.4$. This increase is mainly due to higher FBO$^+$ revenue while FBO$^-$ revenue remains relatively constant. Similar trends occur for higher values of ϵ_p. Finally, considering combined revenues from DBOs and FBOs, smaller ϵ_p values (greater conservativeness in power network constraints) generally lead to higher revenues, while smaller ϵ_s values (greater conservativeness in storage system constraints) reduce revenues.

The results reveal a clear trade-off between conservativeness levels in the power network and storage system constraints. As ϵ_p decreases, the power network requires larger safety margins to mitigate uncertainty, which increases flexibility demands and enhances ESS revenue opportunities. In contrast, decreasing ϵ_s forces the ESS to reserve a larger capacity buffer, limiting its ability to exploit energy arbitrage opportunities, thereby reducing its revenue and, consequently, its investment potential. Thus, the sensitivity of revenues to ϵ highlights the important role of ESS in maintaining operational reliability when participating in market-driven arbitrage. Smaller ϵ_p values increase demand for ESS flexibility within the power network, which boosts its economic value. Conversely, overly conservative storage constraints (ϵ_s too low) limit ESS operational potential, emphasizing the need for balanced risk management in constraint settings.

The synergy between DBO and FBO revenue is particularly notable. For instance, in scenarios like $p0.1 - s0.2$, when DBO revenue is relatively high, FBO revenue tends to be relatively lower. This suggests complementary interactions, where higher DBO revenues partially offset lower FBO revenues. Specifically, as conservativeness in storage constraints becomes relatively higher, the ESS's ability to recover its

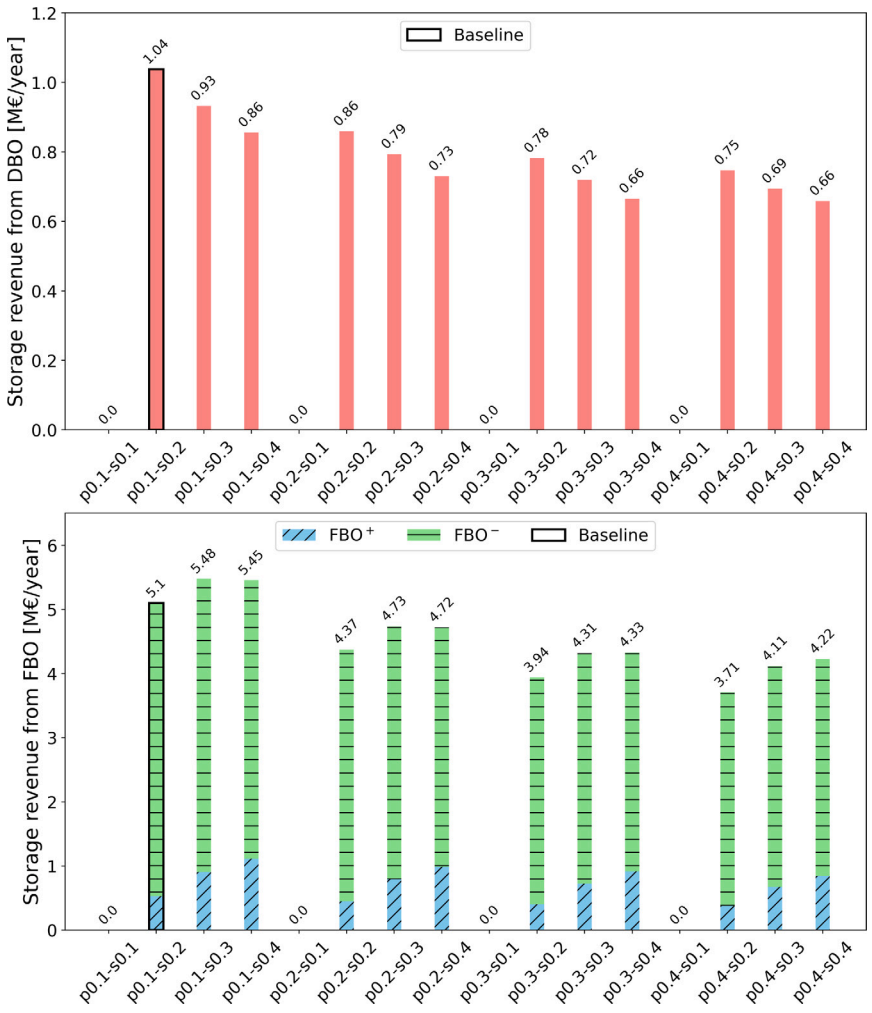

Fig. 8. Sensitivity of ESS revenue from DBOs (top) and FBOs (bottom) to constraint violation probability levels (ϵ) for power network (p) and storage system (s).

investment through RT market arbitrage via FBOs is reduced. Consequently, the system prioritizes further optimizing storage flexibility in the DA market through DBOs. This synergy takes place up to the point where the conservativeness of the ESS constraints becomes too large compared to the revenue potential, making it impossible to recover the investments as shown by the scenarios with $\epsilon_s = 0.1$. These results highlight the importance of jointly optimizing DBO and FBO strategies to maximize total system utility under worst-case wind deviation scenarios while protecting ESS investors from incurring excessive risks in overly conservative settings that could hinder the recovery of their investments.

Lastly, these findings demonstrate the flexibility of the proposed optimization framework, enabling stakeholders to evaluate various ϵ levels and their impact on ESS investment viability and operation. By tailoring the conservativeness of constraints, stakeholders can better align risk tolerances with economic and reliability objectives, paving the way for more effective decision-making in ESS deployment and management.

4.3.2. Energy-to-flexibility spread

Table 3 presents the sensitivity analysis of ESS investments across different configurations of energy-to-flexibility spreads for generators (C_g^{Av}) and storage (C_s^{Av}).

Results show that the total installed ESS power and energy ratings increase as C_g^{Av} and C_s^{Av} rise. When C_s^{Av} increases from 10 to 50 €/MW with C_g^{Av} held constant at 10, the total power and energy ratings grow from 160.41 MW and 145.98 MWh to 243.78 MW and 246.75 MWh,

Table 3
Sensitivity of ESS investment to different energy-to-flexibility spreads for generators (C_g^{Av}) and storage (C_s^{Av}); S1 and S2 denote Storage 1 and Storage 2, respectively.

Metric	C_g^{Av} - C_s^{Av} [€/MW]			
	10–10	10–50	50–10	50–50
Power rating [MW]				
S1	160.41	122.81	185.10	415.67
S2	0.00	120.97	0.00	352.27
Total	160.41	243.78	185.10	767.94
Energy rating [MWh]				
S1	145.98	124.29	168.44	420.17
S2	0.00	122.46	0.00	356.14
Total	145.98	246.75	168.44	776.31
Annualized cost [M€/year]				
S1	6.14	4.95	7.08	16.73
S2	0.00	4.88	0.00	14.18
Total	6.14	9.83	7.08	30.91
Revenue [M€/year]				
S1 (DBO)	1.04	0.81	1.30	1.87
S1 (FBO^+)	0.53	1.21	0.62	5.44
S1 (FBO^-)	4.57	2.93	5.16	9.42
S2 (DBO)	0.00	0.81	0.00	1.69
S2 (FBO^+)	0.00	1.14	0.00	4.10
S2 (FBO^-)	0.00	2.93	0.00	8.39
Total	6.14	9.83	7.08	30.91

respectively, reflecting increases of about 52% and 69%. In contrast, increasing C_g^{Av} from 10 to 50 €/MW with C_s^{Av} held constant at 10 results in only approximately 15% growth in power and energy ratings. This indicates a relatively smaller impact of C_g^{Av} compared to C_s^{Av}. However, when both C_g^{Av} and C_s^{Av} are set to 50 €/MW, (i.e., scenario $50-50$), the total power and energy ratings peak at 767.94 MW and 776.31 MWh, suggesting that their combined effect is greater than their individual impacts. Examining the performance of S1 and S2 separately, S1 consistently shows non-zero ratings, with values increasing as C_g^{Av} rises. In contrast, S2 displays zero ratings when C_g^{Av} is 10, regardless of C_s^{Av}, but shows significant capacity when C_g^{Av} is 50 €/MW. This suggests that S1 is the preferred option unless economic incentives are provided.

The annualized capital costs, calculated by dividing the total investment cost by the system lifetime, and the revenues from DBOs and FBOs exhibit trends consistent with those of the power and energy ratings. The lowest capital cost occurs in scenario $10-10$, increasing to a maximum of 30 M€/year in scenario $50-50$. DBO revenue consistently trails behind FBO revenue, ranging from 11.5% in scenario $50-50$ to 18.4% in scenario $50-10$. Within FBO revenue, FBO^+ is consistently lower than FBO^- across all scenarios. However, FBO^+ revenue becomes significantly higher when C_s^{Av} is set to 50 €/MW. This increase in FBO^+ revenue can be attributed to the fact that as C_s^{Av} rises, ESS revenue also grows, facilitating the installation of additional storage capacity. Consequently, the greater storage capacity allows for enhanced exploitation of temporal energy-to-flexibility arbitrage opportunities in the RT market, leading to a higher revenue stream from FBO^+.

Results indicate that the energy-to-flexibility spread significantly influences ESS investment decisions. Generally, a higher C_g^{Av} encourages increased ESS investment because the higher cost of generator flexibility makes storage a more attractive option. Similarly, a higher C_s^{Av} promotes greater ESS participation. Although a higher C_s^{Av} raises the cost of flexibility from storage, this is offset by the benefits of using ESS as a flexibility provider instead of relying on generators. With an effective pricing mechanism and sufficient ESS capacity installed, the system can allocate more flexibility to storage in the RT market, reducing reliance on generator flexibility and optimizing generation dispatch in the DA market. This results in enhanced social welfare and overall system resilience. However, this effect may diminish if the energy-to-flexibility spread becomes too large relative to the DA market price. Ultimately, the results demonstrate that the proposed approach enables investment recovery through revenues obtained from DBOs and FBOs, highlighting the financial viability of ESS across various scenarios. While the specific impact of different spread settings is notable, the revenue stream from FBOs remains a crucial factor for ESS investment recovery, highlighting the potential benefits of integrating the proposed flexibility block orders into the current electricity market structure.

5. Conclusion

In this paper, we consider a generic optimal energy storage planning problem for a power transmission system characterized by a high penetration of wind power generation. The problem seeks to maximize the utility of the power system while compensating for possible power imbalances resulting from imperfect wind forecasts. The problem is formulated as a data-driven DRCC program. To facilitate renewable energy integration, the storage system acts as a flexibility provider in both the DA and RT market segments along with flexible generating units. The operation of the storage system is governed by two new market products, namely (1) DA Block Orders (DBOs) and (2) Flexibility Block Orders (FBOs) designed to hedge ESS investors against uncertainties without jeopardizing the competitiveness of the market. Extensive numerical simulation allows us to draw the following conclusions:

1. The proposed energy storage planning problem allows for the development of a storage investment strategy that meets the needs of system operators by addressing worst-case wind deviations while ensuring investment recovery for investors.
2. The novel DBOs and FBOs introduced in this study demonstrate their effectiveness in enabling the storage system to capitalize on opportunities within the electricity market while mitigating risks associated with forecast errors.
3. Through the adoption of the DRCC framework, different stakeholders (i.e., regulators, and private investors) can assess various violation probability levels to comprehend their impact on the optimal storage capacity configuration. This enables informed decision-making aligned with their specific requirements.
4. Under specified conditions, integrating a 146 MWh Energy Storage System with a 1:1 energy-to-power ratio enhances system utility by efficiently mitigating wind power mismatch. The total investment is 61.6 M€, with 16.9% recovered through DA arbitrage (DBOs) and 83.1% through RT arbitrage (FBOs), emphasizing the value of capitalizing on opportunities in the RT market.
5. Sensitivity analysis reveals that the energy-to-flexibility spread greatly affects the optimal strategy, with higher spreads enhancing ESS flexibility. Varying the constraint violation probability (ϵ) shows a trade-off between robustness and economic performance, highlighting the potential downsides of excessive conservativeness on ESS decisions. Despite different hyperparameter settings, the revenue from FBOs in the RT market remains a crucial factor for ESS investment recovery.

In conclusion, our study emphasizes the need for flexible financial instruments to enhance investment in ESS. We show how customized products, such as block orders, can overcome market limitations and mitigate risks from forecasting errors. This approach has the potential to increase revenue for ESS investors, thereby supporting renewable energy integration, and improving grid stability. Future research should refine these models by incorporating more detailed technology modelling and exploring innovative market products to further stimulate private investment, promoting the development of a more resilient and efficient energy system.

CRediT authorship contribution statement

A. Belmondo Bianchi: Writing – review & editing, Writing – original draft, Visualization, Validation, Software, Methodology, Investigation, Formal analysis, Data curation, Conceptualization. **H.H.M. Rijnaarts:** Writing – review & editing, Supervision, Resources, Project administration, Funding acquisition. **S. Shariat Torbaghan:** Writing – review & editing, Writing – original draft, Validation, Supervision, Resources, Project administration, Methodology, Investigation, Funding acquisition, Conceptualization.

Declaration of competing interest

The authors declare that they have no known competing financial interests or personal relationships that could have appeared to influence the work reported in this paper.

Acknowledgements

This research was performed within the framework of the research program AquaConnect, funded by the Dutch Research Council (NWO, grant-ID P19-45) and public and private partners of the AquaConnect consortium and coordinated by Wageningen University and Research, Netherlands.

Data availability

Data has been made available in the online appendix [57].

References

[1] J. Jasiūnas, P.D. Lund, J. Mikkola, Energy system resilience–A review, Renew. Sustain. Energy Rev. 150 (2021) 111476.

[2] D. Azari, S.S. Torbaghan, M. Gibescu, M.A. Van Der Meijden, The impact of energy storage on long term transmission planning in the north sea region, in: 2014 North American Power Symposium, NAPS, IEEE, 2014, pp. 1–6.

[3] M. Beaudin, H. Zareipour, A. Schellenberglabe, W. Rosehart, Energy storage for mitigating the variability of renewable electricity sources: An updated review, Energy Sustain. Develop. 14 (4) (2010) 302–314.

[4] M. Stecca, L.R. Elizondo, T.B. Soeiro, P. Bauer, P. Palensky, A comprehensive review of the integration of battery energy storage systems into distribution networks, IEEE Open J. Ind. Electron. Soc. 1 (2020) 46–65.

[5] N. Mararakanye, B. Bekker, Renewable energy integration impacts within the context of generator type, penetration level and grid characteristics, Renew. Sustain. Energy Rev. 108 (2019) 441–451.

[6] C.N. Dimitriadis, E.G. Tsimopoulos, M.C. Georgiadis, Optimization-based economic analysis of energy storage technologies in a coupled electricity and natural gas market, J. Energy Storage 58 (2023) 106332.

[7] Z. Chen, L. Wu, Y. Fu, Real-time price-based demand response management for residential appliances via stochastic optimization and robust optimization, IEEE Trans. Smart Grid 3 (4) (2012) 1822–1831.

[8] H. Zhong, L. Xie, Q. Xia, Coupon incentive-based demand response: Theory and case study, IEEE Trans. Power Syst. 28 (2) (2012) 1266–1276.

[9] G. Tsaousoglou, A new notion of reserve for power systems with high penetration of storage and flexible demand, IEEE Trans. Energy Mark. Policy Regul. (2023).

[10] X. Wu, J. Zhao, A.J. Conejo, Optimal battery sizing for frequency regulation and energy arbitrage, IEEE Trans. Power Deliv. 37 (3) (2021) 2016–2023.

[11] H. Ding, P. Pinson, Z. Hu, Y. Song, Integrated bidding and operating strategies for wind-storage systems, IEEE Trans. Sustain. Energy 7 (1) (2015) 163–172.

[12] T. Zonjee, S.S. Torbaghan, Energy storage arbitrage in day-ahead electricity market using deep reinforcement learning, in: 2023 IEEE Belgrade PowerTech, IEEE, 2023, pp. 1–7.

[13] E. Côté, S. Salm, Risk-adjusted preferences of utility companies and institutional investors for battery storage and green hydrogen investment, Energy Policy 163 (2022) 112821.

[14] J. Haas, F. Cebulla, K. Cao, W. Nowak, R. Palma-Behnke, C. Rahmann, P. Mancarella, Challenges and trends of energy storage expansion planning for flexibility provision in low-carbon power systems–a review, Renew. Sustain. Energy Rev. 80 (2017) 603–619.

[15] M.E. Ölmez, I. Ari, G. Tuzkaya, A comprehensive review of the impacts of energy storage on power markets, J. Energy Storage 91 (2024) 111935.

[16] P. Pinson, L. Han, J. Kazempour, Regression markets and application to energy forecasting, Top 30 (3) (2022) 533–573.

[17] L. Miller, R. Carriveau, A review of energy storage financing—Learning from and partnering with the renewable energy industry, J. Energy Stor. 19 (2018) 311–319.

[18] C. Sweeney, R.J. Bessa, J. Browell, P. Pinson, The future of forecasting for renewable energy, Wiley Interdiscip. Rev.: Energy Environ. 9 (2) (2020) e365.

[19] M. Bulut, E. Özcan, How to build a state-of-the-art battery energy storage market? Challenges, opportunities, and future directions, J. Energy Storage 86 (2024) 111174.

[20] F. Rahman, S. Rehman, M.A. Abdul-Majeed, Overview of energy storage systems for storing electricity from renewable energy sources in Saudi Arabia, Renew. Sustain. Energy Rev. 16 (1) (2012) 274–283.

[21] J. Schoonderwoerd, A.B. Bianchi, T. Zonjee, W.-S. Chen, S.S. Torbaghan, Hydrogen production from non-potable water resources: A techno-economic investment and operation planning approach, J. Clean. Prod. 473 (2024) 143501.

[22] H. Zhao, Q. Wu, S. Hu, H. Xu, C.N. Rasmussen, Review of energy storage system for wind power integration support, Appl. Energy 137 (2015) 545–553.

[23] M. Numan, M.F. Baig, M. Yousif, et al., Reliability evaluation of energy storage systems combined with other grid flexibility options: A review, J. Energy Storage 63 (2023) 107022.

[24] W.B. Powell, Reinforcement Learning and Stochastic Optimization: A Unified Framework for Sequential Decisions, John Wiley & Sons, 2022.

[25] C.H. Hao, P.K. Wesseh Jr., J. Wang, H. Abudu, K.E. Dogah, D.I. Okorie, E.E.O. Opoku, Dynamic pricing in consumer-centric electricity markets: A systematic review and thematic analysis, Energy Strategy Rev. 52 (2024) 101349.

[26] S. Zhan, P. Hou, G. Yang, J. Hu, Distributionally robust chance-constrained flexibility planning for integrated energy system, Int. J. Electr. Power Energy Syst. 135 (2022) 107417.

[27] J. Li, W. Wang, Z. Yuan, J. Chen, Y. Zhang, Optimal multi-market operation of gravity energy storage and wind power producer using a hybrid stochastic/robust optimization, J. Energy Storage 68 (2023) 107760.

[28] D. Cremoncini, G.F. Frate, A. Bischi, T.T. Pedersen, G.B. Andresen, A. Bentien, L. Ferrari, Optimal participation of a wind and hybrid battery storage system in the day-ahead and automatic frequency restoration reserve markets, J. Energy Storage 94 (2024) 112309.

[29] S.S. Parvar, H. Nazaripouya, Optimal operation of battery energy storage under uncertainty using data-driven distributionally robust optimization, Electr. Power Syst. Res. 211 (2022) 108180.

[30] S. Bhattacharjee, R. Sioshansi, H. Zareipour, Energy storage participation in wholesale markets: The impact of state-of-energy management, IEEE Open Access J. Power Energy 9 (2022) 173–182.

[31] M. Dadashi, K. Zare, H. Seyedi, M. Shafie-khah, Coordination of wind power producers with an energy storage system for the optimal participation in wholesale electricity markets, Int. J. Electr. Power Energy Syst. 136 (2022) 107672.

[32] A.B. Bianchi, J. Willet, H. Rijnaarts, S.S. Torbaghan, Distribution robust water-based demand side management in power transmission networks, Sustain. Energy Grids Netw. 36 (2023) 101232.

[33] L. Roald, F. Oldewurtel, B. Van Parys, G. Andersson, Security constrained optimal power flow with distributionally robust chance constraints, 2015, arXiv preprint arXiv:1508.06061.

[34] X. Zheng, M.E. Khodayar, J. Wang, M. Yue, A. Zhou, Distributionally robust multistage dispatch with discrete recourse of energy storage systems, IEEE Trans. Power Syst. (2024).

[35] A. Valencia, R.A. Hincapie, R.A. Gallego, Optimal location, selection, and operation of battery energy storage systems and renewable distributed generation in medium–low voltage distribution networks, J. Energy Storage 34 (2021) 102158.

[36] R. Xie, W. Wei, M. Li, Z. Dong, S. Mei, Sizing capacities of renewable generation, transmission, and energy storage for low-carbon power systems: A distributionally robust optimization approach, Energy 263 (2023) 125653.

[37] J. Li, Z. Xu, H. Liu, C. Wang, L. Wang, C. Gu, A Wasserstein distributionally robust planning model for renewable sources and energy storage systems under multiple uncertainties, IEEE Trans. Sustain. Energy (2022).

[38] M. Karasavvidis, D. Papadaskalopoulos, G. Strbac, Optimal offering of a power producer in electricity markets with profile and linked block orders, IEEE Trans. Power Syst. 37 (4) (2021) 2704–2719.

[39] N.E. Koltsaklis, I. Zenginis, A.S. Dagoumas, Assessing new block order options of the EUPHEMIA algorithm: An optimization model for the economic dispatch problem in power exchanges, Energy Rep. 6 (2020) 3119–3140.

[40] EPEX SPOT, EPEX SPOT introduces curtailable blocks and loop blocks in all day-ahead markets, 2018, URL: https://www.epexspot.com/en/news/epex-spot-introduces-curtailable-blocks-and-loop-blocks-all-day-ahead-markets. (Accessed: 10 July 2024).

[41] Nemo Committee, et al., EUPHEMIA public description: Single price coupling algorithm, 2024, URL: https://www.nordpoolgroup.com/globalassets/download-center/single-day-ahead-coupling/EUPHEMIA-public-description.pdf.

[42] A.E. El Adlani, J.M. Riquelme-Santos, C. Gómez-Quiles, A decomposition-based approach to European electricity market clearing, Int. J. Electr. Power Energy Syst. 161 (2024) 110192.

[43] S.S. Torbaghan, M. Madani, P. Sels, A. Virag, H. Le Cadre, K. Kessels, Y. Mou, Designing day-ahead multi-carrier markets for flexibility: Models and clearing algorithms, Appl. Energy 285 (2021) 116390.

[44] MAGNITUDE Project, Specification of the multi-energy market simulator, 2019, https://www.magnitude-project.eu/results-and-publications/main-results-including-public-deliverables/. (Accessed: 05 December 2024).

[45] A. Arrigo, C. Ordoudis, J. Kazempour, Z. De Grève, J.-F. Toubeau, F. Vallée, Wasserstein distributionally robust chance-constrained optimization for energy and reserve dispatch: An exact and physically-bounded formulation, European J. Oper. Res. 296 (1) (2022) 304–322.

[46] Q. Fan, D. Liu, A Wasserstein-distance-based distributionally robust chance constrained bidding model for virtual power plant considering electricity-carbon trading, IET Renew. Power Gener. 18 (3) (2024) 545–557.

[47] L.A. Roald, D. Pozo, A. Papavasiliou, D.K. Molzahn, J. Kazempour, A. Conejo, Power systems optimization under uncertainty: A review of methods and applications, Electr. Power Syst. Res. 214 (2023) 108725.

[48] D. Feldman, V. Ramasamy, R. Fu, A. Ramdas, J. Desai, R. Margolis, US Solar Photovoltaic System and Energy Storage Cost Benchmark (Q1 2020), Technical Report, National Renewable Energy Lab.(NREL), Golden, CO (United States), 2021.

[49] W. Cole, A.W. Frazier, C. Augustine, Cost Projections for Utility-Scale Battery Storage: 2021 Update, Technical Report, National Renewable Energy Lab.(NREL), Golden, CO (United States), 2021.

[50] F. Pourahmadi, J. Kazempour, Distributionally robust generation expansion planning with unimodality and risk constraints, IEEE Trans. Power Syst. 36 (5) (2021) 4281–4295.

[51] A. Ratha, A. Schwele, J. Kazempour, P. Pinson, S.S. Torbaghan, A. Virag, Affine policies for flexibility provision by natural gas networks to power systems, Electr. Power Syst. Res. 189 (2020) 106565.

[52] G.A. Hanasusanto, V. Roitch, D. Kuhn, W. Wiesemann, A distributionally robust perspective on uncertainty quantification and chance constrained programming, Math. Program. 151 (1) (2015) 35–62.

[53] H. Rahimian, S. Mehrotra, Distributionally robust optimization: A review, 2019, arXiv preprint arXiv:1908.05659.
[54] K. Baker, E. Dall'Anese, T. Summers, Distribution-agnostic stochastic optimal power flow for distribution grids, in: 2016 North American Power Symposium, NAPS, IEEE, 2016, pp. 1–6.
[55] W. Xie, S. Ahmed, Distributionally robust chance constrained optimal power flow with renewables: A conic reformulation, IEEE Trans. Power Syst. 33 (2) (2017) 1860–1867.
[56] C. Ordoudis, P. Pinson, J.M. Morales, M. Zugno, An updated version of the IEEE RTS 24-bus system for electricity market and power system operation studies, 13, 2016, Technical University of Denmark.
[57] A. Belmondo Bianchi, Uncertainty-aware energy storage investment planning through arbitrage in DA and RT markets using novel block orders, 2024, http://dx.doi.org/10.17632/j3wmg49m23.1, Mendeley Data.
[58] L. Hirth, J. Mühlenpfordt, M. Bulkeley, The ENTSO-e transparency platform–A review of Europe's most ambitious electricity data platform, Appl. Energy 225 (2018) 1054–1067.
[59] J.E.B. Iversen, P. Pinson, Resgen: Renewable energy scenario generation platform, in: 2016 IEEE Power Engineering Society General Meeting, IEEE, 2016, pp. 1–5.